iScience

CellPress
OPEN ACCESS

Article

Increased muscle coactivation is linked with fast feedback control when reaching in unpredictable visual environments

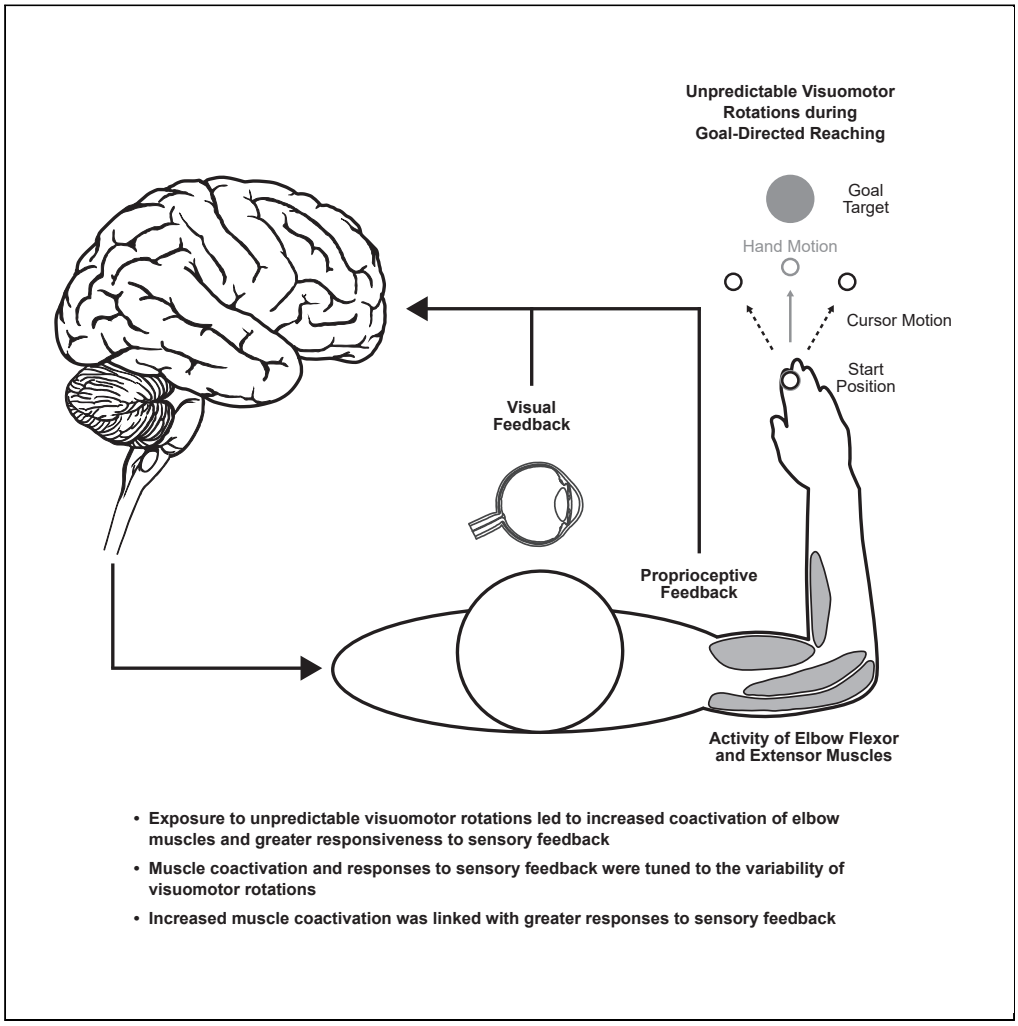

Philipp Maurus, Ghadeer Mahdi, Tyler Cluff

tyler.cluff@ucalgary.ca

Highlights

Participants encountered unpredictable visuomotor rotations during reaching

Exposure led to increased muscle coactivation and responses to sensory feedback

Coactivation and responses to feedback scaled with the variability of the rotations

Increased coactivation was linked with greater corrective responses to feedback

Maurus et al., iScience 27, 111174
November 15, 2024
https://doi.org/10.1016/j.isci.2024.111174

iScience

CellPress
OPEN ACCESS

Article

Increased muscle coactivation is linked with fast feedback control when reaching in unpredictable visual environments

Philipp Maurus,[1] Ghadeer Mahdi,[1] and Tyler Cluff[1,2,3,*]

SUMMARY

Humans encounter unpredictable disturbances in daily activities and sports. When encountering unpredictable physical disturbances, healthy participants increase the peak velocity of their reaching movements, muscle coactivation, and responses to sensory feedback. Emerging evidence suggests that muscle coactivation may facilitate responses to sensory feedback and may not solely increase stiffness to resist displacements. We tested this idea by examining how healthy participants alter the control of reaching movements and responses to sensory feedback when encountering variable visuomotor rotations. The rotations changed amplitude and direction between movements, creating unpredictable errors that required fast online corrections. Participants increased the peak velocity of their movements, muscle coactivation, and responses to visual and proprioceptive feedback with the variability of the visuomotor rotations. The findings highlight an increase in neural responsiveness to sensory feedback and suggest that muscle coactivation may prime the nervous system for fast responses to sensory feedback that accommodate properties of unpredictable visual environments.

INTRODUCTION

Humans can encounter unpredictable disturbances as they perform activities of daily living. Disturbances may arise if bumped and thrown off balance while navigating a busy sidewalk. They are also prevalent in sports. Consider a tennis player receiving a serve, where the spin of the ball may cause it to change trajectory unexpectedly in gusting winds. Variations in the amplitude and direction of these disturbances are difficult to anticipate and have the potential to impair task performance.

Several studies have examined how healthy human participants alter their reaching movements when they encounter unpredictable mechanical disturbances. These disturbances may arise from the abrupt exposure to a novel physical load or physical disturbances that can vary in amplitude and direction within or between movements.[1–8] A common finding across a range of reaching tasks is that healthy adults produce more vigorous movements when they encounter variable physical disturbances. They coactivate pairs of agonist and antagonist muscles,[1–5] increase the peak velocity of their reaching movements,[4–6] grip handheld objects more forcefully,[7] and become more responsive to proprioceptive and visual feedback.[1,2,4,5] Increases in the vigor of reaching movements and responses to sensory feedback parallel the variability of the unpredictable physical disturbances.[5–7]

Increases in responsiveness to sensory feedback may enable the nervous system to deal with errors imposed by unpredictable physical disturbances. Optimal feedback control has become a central theory for interpreting the importance of sensory feedback in biological movement.[9–13] The theory offers a benchmark for interpreting voluntary actions and a range of strategies that prioritize different features of movement.[4,5,14] Central to the theory is the idea of a control policy that transforms sensory feedback into motor commands that are optimal for attaining the goal of the task.[9–13] When moving in variable environments, the theory predicts that the best solution for maintaining performance is to make the control policy as robust and insensitive to disturbances as possible.[4,5,14] Recent work has proposed that the nervous system alters its control strategy to become more robust to physical disturbances that are variable and difficult to anticipate.[4,5,14] The change in control strategy is linked with a general increase in responsiveness to visual and proprioceptive feedback.[5] Emerging evidence suggests that muscle coactivation may help to amplify neural responses to sensory feedback by increasing excitation of the agonist muscles, inhibiting the antagonist muscles, or engaging both muscles for online control.[4,5,11] Indeed, instructions to coactivate their muscles enable participants to produce larger muscle responses and return faster to specific arm and body postures when responding to the same physical disturbances.[15,16]

Muscle coactivation may also leverage intrinsic muscle properties to stiffen the arm and provide instantaneous resistance to physical disturbances.[3,17–22] The nervous system is thought to set muscle coactivation, and thus stiffness, independently from responses to sensory

[1]Faculty of Kinesiology, University of Calgary, Calgary, AB T2N 1N4, Canada
[2]Hotchkiss Brain Institute, University of Calgary, Calgary, AB T2N 1N4, Canada
[3]Lead contact
*Correspondence: tyler.cluff@ucalgary.ca
https://doi.org/10.1016/j.isci.2024.111174

feedback.[18,23–25] However, it is challenging to estimate muscle stiffness *in vivo* because the initial motion of the arm is dominated by its inertia following physical disturbances.[26] As a result, muscle stiffness has been estimated in time windows where multiple neural feedback loops are engaged in control.[12,27,28] It is difficult to disentangle contributions from intrinsic muscle stiffness that resists physical disturbances and the potential interplay between muscle coactivation and neural responses to sensory feedback.

Visual disturbances may provide a means to test the generality of the changes in control that occur when moving in variable environments and insight into the relationship between muscle coactivation and responsiveness to sensory feedback. It is clear that humans and non-human primates coactivate their muscles when they are abruptly exposed to a novel visuomotor rotation.[29,30] It is still unclear whether the nervous system tunes control to the variability of unpredictable visual disturbances and benefits from muscle coactivation when responding to visual disturbances. In contrast to physical disturbances, visual disturbances do not benefit from muscle stiffness since they do not impose any physical displacements that require participants to resist against (cf.[30]). Instead, visual disturbances necessitate neural control to rapidly engage in corrective responses and complete movements within the time demands of the task. As a result, visual disturbances provide a direct probe of the neural control policy and a means to assess the relationship between muscle coactivation, neural responses to sensory feedback, and the resulting behavioral corrections. If muscle coactivation increases the nervous system's responsiveness to sensory feedback, it should emerge spontaneously to facilitate responses to unpredictable visual disturbances.

Here, we tested how the nervous system alters the control of reaching movements in the presence of unpredictable visual disturbances. We sought to address the question of how the nervous system alters feedback gains when exposed to variable visual disturbances and understand how muscle coactivation may be involved in generating these responses. We examined these questions by exposing healthy participants to visuomotor rotations that altered the mapping between the motion of their occluded hand and a feedback cursor displayed in their workspace. The visuomotor rotations created unpredictable cursor deviations by changing in direction and amplitude between movements. The task imposed larger errors by exposing participants to larger and more variable cursor rotations. The random nature of these disturbances requires that participants generate larger corrections to complete their movements within the timing demands of the task. Across three experiments, we show that participants increase the peak velocities of their reaching movements, coactivate their muscles, and show a global increase in responsiveness to visual and proprioceptive feedback when exposed to more variable visual disturbances. The findings highlight an increase in neural responsiveness to sensory feedback and suggest that muscle coactivation may play an important role in priming the nervous system for fast responses to sensory feedback to accommodate the properties of unpredictable visual environments.

RESULTS

Goal-directed reaching movements in the absence or presence of unpredictable visuomotor rotations

Healthy human participants (N = 90, 45 females, 45 males, 18–38 years, 3 left-handed) performed goal-directed reaching movements with their dominant arm in one of three experiments. The experiments were performed while seated in a robotic exoskeleton that supports the arm and allows participants to make planar movements in a near frictionless environment. The robot is capable of applying independent loads to the shoulder and/or elbow joints[31,32] and is paired with a visual display that projects targets and a feedback cursor (1 cm diameter) into the participant's workspace via a semi-silvered mirror (see STAR Methods for full details). Direct vision of the hand and arm was occluded by a metal barrier throughout the experiments. We recorded the activity of two monoarticular (brachioradialis and triceps lateralis) and two biarticular (biceps and triceps longus) elbow muscles using surface electromyography.

Participants had to move their feedback cursor from a start position into a goal target within 500–700 ms after initiating their movement (Figures 1A and 1B). They received explicit visual feedback about the timing of their movements while holding the goal target at the end of each trial (see STAR Methods). The experiments were divided into baseline, exposure, and washout phases. Movements in the baseline and washout phases were performed with veridical visual feedback where the cursor was tethered to the motion of the participant's finger. Movements in the exposure phase were performed in the presence of unpredictable visuomotor rotations (VMRs; Figure 1C). The VMRs altered the mapping between the position of the participants' hand and a feedback cursor displayed in their workspace. The amplitude and direction of the rotations could change between trials. Thus, participants were unable to anticipate the visual disturbances and had to generate rapid feedback responses to mobilize their arm, counter the rotations, and complete their movements successfully. We modified the absolute amplitude of the VMRs to impose larger and more variable disturbances in separate blocks of the exposure phase (Figures 1C and 1D). Changes in voluntary reaching behavior were examined in unperturbed trials (i.e., absence of VMRs) that were randomly interleaved during the exposure phase. Throughout each experiment, neural feedback gains were probed using cursor jump perturbations ($\pm$4 cm) applied at the onset of randomly selected trials (Figure 1B, see STAR Methods for full details).[2,5,33,34] The rotations were not applied in cursor jump trials, providing a direct assessment of how the nervous system's responsiveness to the same visual probes changed throughout the experiment. The task design enabled us to examine changes in voluntary reaching movements and responses to sensory feedback when moving in environments that imposed variable visual errors and required rapid corrections to complete movements within the timing demands of the task.

Exposure to unpredictable visual disturbances increases the vigor of voluntary reaching movements, muscle coactivation, and responsiveness to visual feedback

Experiment 1 examined changes in coactivation and responsiveness to sensory feedback when moving in unpredictable visual environments. Participants (N = 30) performed goal-directed reaching movements in the absence (baseline and washout) or presence (exposure phase) of VMRs with different levels of variability ($\pm$20° and $\pm$30°; Figures 1B–1D). We first examined how participants altered their voluntary reaching

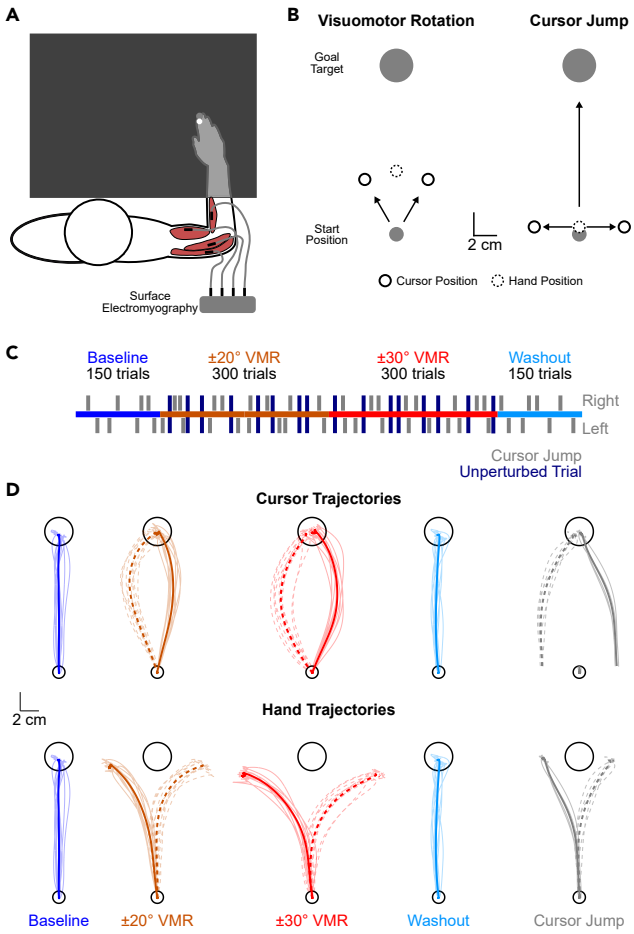

Figure 1. General task description

(A) Participants performed goal-directed reaching movements with their dominant arm supported in a robotic exoskeleton. The activity of the monoarticular elbow muscles and biarticular muscles was recorded with surface electromyography.

(B) Participants performed reaching movements in the absence or presence of variable visuomotor rotations (VMRs). The VMRs rotated the feedback cursor clockwise or counterclockwise relative to the hand in random order. Lateral cursor jumps (±4 cm) were used to probe the responsiveness to visual feedback in random trials throughout the experiment. The cursor jumped laterally when the participant left the start position (i.e., movement onset). The rotations were not applied in cursor jump trials.

(C) *Experiment 1* included baseline, exposure, and washout phases. Participants encountered unpredictable visuomotor rotations with different levels of variability in separate subphases of the exposure phase (±20° and ±30°). In addition to cursor jumps, unperturbed trials (absence of visuomotor rotations) were also randomly interleaved during the exposure phase.

(D) Exemplary cursor and hand trajectories performed by a representative participant in the absence (baseline and washout) or presence of unpredictable VMRs in *Experiment 1*. Gray lines indicate cursor jump trials. The unpredictable VMRs elicit lateral cursor displacements and require corrections of the hand trajectory. Thick lines represent the average cursor and hand trajectories. Thin lines are individual trials. Counterclockwise rotations (dashed lines) required clockwise corrections of the hand trajectory and vice versa. Similarly, rightward cursor jumps required leftward corrections of the hand trajectory and vice versa.

movements when exposed to the cursor rotations. We used the peak forward hand velocity as a measure of movement vigor and proxy for the feedback gains during unperturbed movements.[4,5,14] Figure 2A displays the forward hand velocities across phases of the experiment. We expected that participants would display similar changes in reaching as observed in unpredictable mechanical environments,[5,6] including an increase in their peak forward velocities that parallels the variability of the VMRs. We used contrast analyses to test this prediction (extended linear trends; see STAR Methods for details).[35–37] Indeed, participants displayed an increase in peak forward hand velocities that was most prominent when encountering more variable VMRs ($\Delta\bar{x}$ = 1.5 cm/s, 95% confidence interval [CI] [0.7, 2.3], t(29) = 3.79, $p < 0.001$, d = 0.8). The timing of the peak velocities also shifted to earlier in the movement when participants encountered more variable VMRs ($\Delta\bar{x}$ = 16 ms, 95% CI [7, 24], t(29) = 3.88, $p < 0.001$, d = 0.5). Movement times did not differ statistically across phases of the experiment ($\Delta\bar{x}$ = 7 ms, 95% CI [−10, 23], t(29) = 0.82, $p = 0.417$, d = 0.2), which rules out the explanation that participants increased their feedback gains by planning for movements with shorter duration.[38]

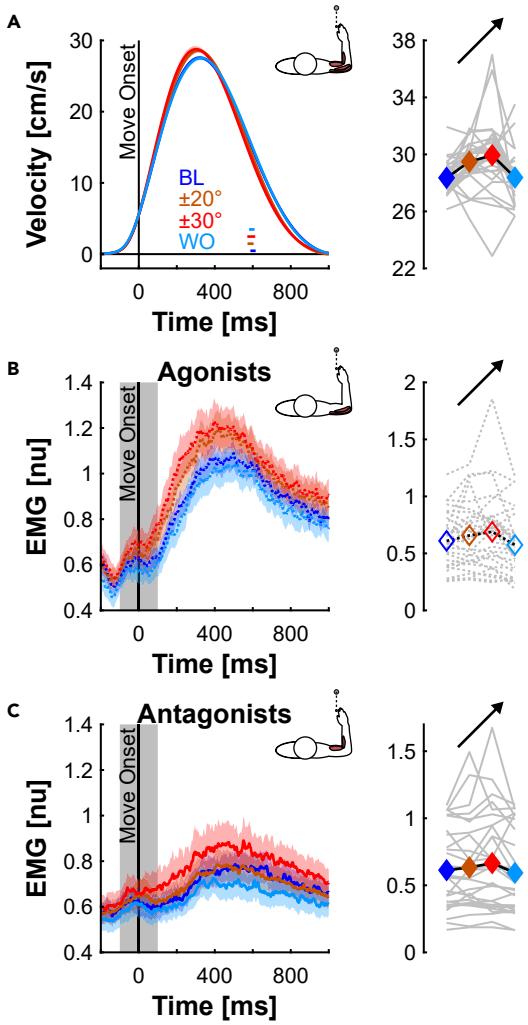

Figure 2. Properties of voluntary behavior and associated muscle activity of unperturbed trials in *Experiment 1*

(A) Group mean ± SE forward velocities in each phase of the experiment. The data are aligned with movement onset (t = 0 ms). Colored horizontal lines indicate the 95% confidence interval of the movement time across phases of the experiment. The side panel displays each individual's mean peak forward velocity (gray lines) and the corresponding group means (colored diamonds and black line) across experimental phases.

(B) Group mean ± SE activity of the elbow extensor muscles (solid lines) plotted in the same format as (A). The data were smoothed with a 10 sample (10 ms), zero-delay moving average for display purposes. The shaded, gray area (−100 to 100 ms) indicates the muscle activity associated with the planning and initiation of voluntary behavior. The side panel displays the average muscle activity surrounding movement onset.

(C) Group mean ± SE activity of the elbow flexor muscles (dashed lines) plotted in the same format as (B).

Arrows indicate statistically significant contrasts. BL, baseline; WO, washout; nu, normalized unit.

We further assayed voluntary behavior by extracting the average activity of the elbow muscles surrounding the onset of unperturbed movements with veridical visual feedback (−100 to 100 ms; Figures 2B and 2C).[5,39–43] Note that we pooled the activity of the mono- and biarticular muscles since similar changes in activity were observed across these synergistic muscles (see STAR Methods).[5,44] Separate averages were then calculated for the elbow flexor and extensor muscles. We expected that participants would increase the activity of their elbow muscles in parallel with the variability of the unpredictable VMRs similar to changes in muscle activity that have been observed in unpredictable mechanical environments.[4,5] In line with this prediction, participants increased the activity of both the elbow flexor and extensor muscles in the exposure phase. Increases in elbow muscle activity were most prominent when encountering more variable visual disturbances (flexors: $\Delta\bar{x}$ = 0.06 normalized unit [nu], 95% CI [0.01, 0.10], t(29) = 2.59, p = 0.015, d = 0.2; extensors: $\Delta\bar{x}$ = 0.09 nu, 95% CI [0.04, 0.14], t(29) = 3.66, p < 0.001, d = 0.3). Collectively, the findings reveal an increase and shift in peak movement velocities to earlier in movement paired with increases in muscle coactivation when reaching in the presence of more variable VMRs.

We then examined how the nervous system's responsiveness to visual feedback changed throughout the experiment. Participants encountered randomly interleaved trials in which the position of the feedback cursor shifted abruptly by 4 cm to the left or right of the target at the

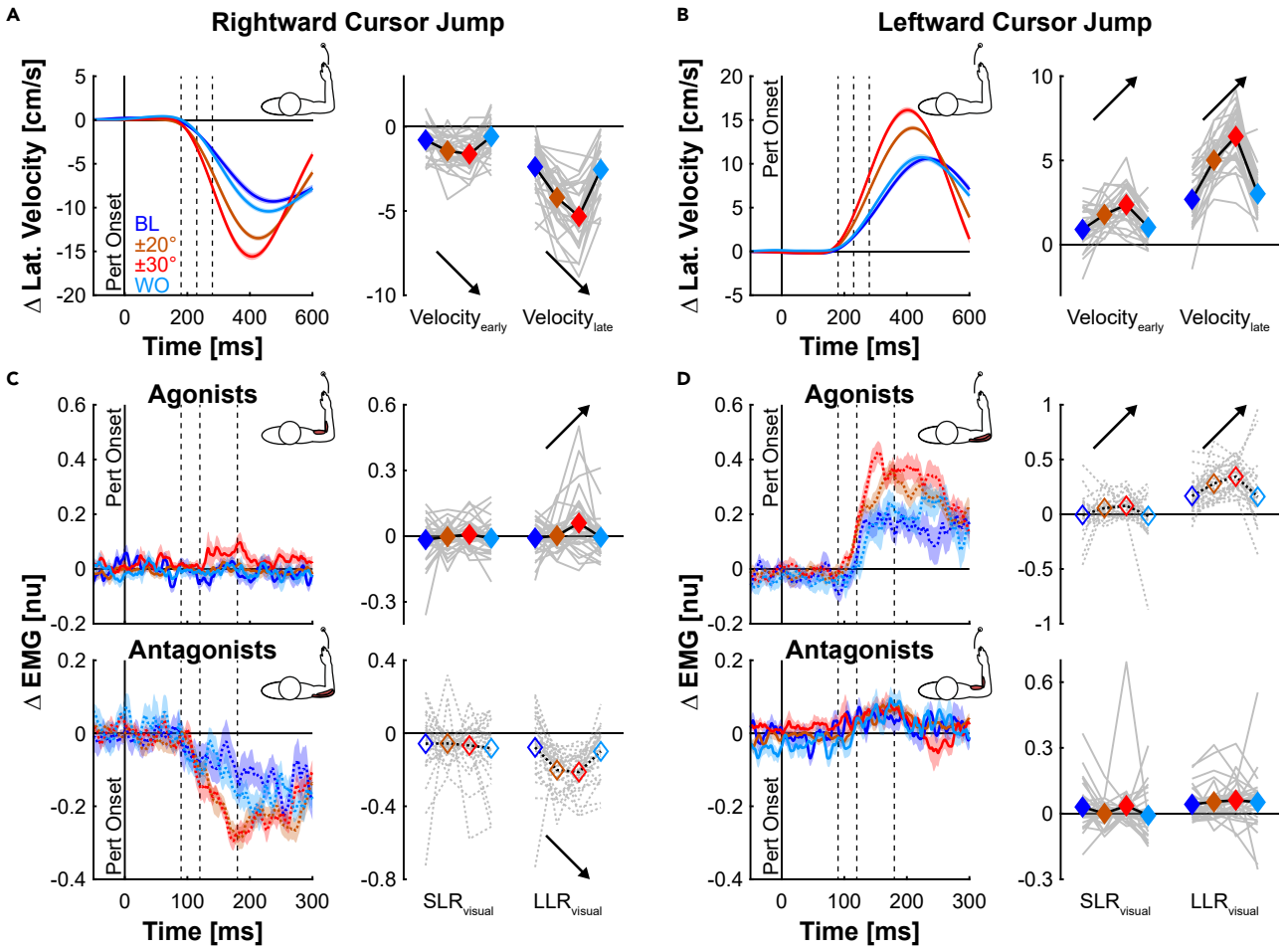

Figure 3. Lateral velocities and muscle responses during visual probes in *Experiment 1*

(A) Group mean ± SE change in lateral velocities in each phase of the experiment during rightward cursor jumps. The data are aligned with the onset of the visual probes (t = 0 ms). The dashed, vertical lines separate the velocity$_{early}$ (180–230 ms) and velocity$_{late}$ (230–280 ms) time windows. The side panel displays the mean lateral velocity in the velocity$_{early}$ and velocity$_{late}$ time windows for each participant (gray lines) across experimental phases. The colored diamonds and black line represent the group means.

(B) Group mean ± SE change in lateral velocities in each phase of the experiment during leftward cursor jumps plotted in the same format as (A).

(C) Group mean ± SE change in activity of the elbow flexor (solid lines, upper panel) and extensor muscles (dashed lines, lower panel) during rightward cursor jumps. The data are aligned with the onset of the visual probe (t = 0 ms). The dashed, vertical lines separate the SLR$_{visual}$ (90–120 ms) and LLR$_{visual}$ (120–180 ms). The data were smoothed with a 10 sample (10 ms), zero-delay moving average for display purposes. The side panels display the mean muscle activity in the SLR$_{visual}$ and LLR$_{visual}$ time windows for the elbow flexors (solid gray lines, upper panel) and extensors (dashed gray lines, lower panel) for each participant across experimental phases. The colored diamonds and black line represent the group means.

(D) Group mean ± SE change in activity of the elbow extensor (dashed lines, upper panel) and flexor muscles (solid lines, lower panel) during leftward cursor jumps plotted in the same format as (C).

Arrows indicate statistically significant contrasts. BL, baseline; WO, washout; nu, normalized unit.

onset of movement (see STAR Methods for more details). We predicted that participants would increase the velocity of their corrective responses in parallel with the variability of the imposed VMRs. Figures 3A and 3B display the lateral velocities during rightward and leftward visual probes. In agreement with the prediction, participants increased the lateral velocity of their corrective responses to the same visual probes when interacting with more variable VMRs. Increased lateral velocities were evident in both the early (right: $\Delta\bar{x}$ = 0.9 cm/s, 95% CI [0.5, 1.3], t(29) = 4.37, $p < 0.001$, d = 0.9; left: $\Delta\bar{x}$ = 1.3 cm/s, 95% CI [1.0, 1.7], t(29) = 7.83, $p < 0.001$, d = 1.3) and late response windows (right: $\Delta\bar{x}$ = 2.7 cm/s, 95% CI [2.2, 3.2], t(29) = 10.37, $p < 0.001$, d = 1.8; left: $\Delta\bar{x}$ = 3.3 cm/s, 95% CI [2.9, 3.8], t(29) = 16.46, $p < 0.001$, d = 2.4).

We gained insight into the neural implementation of the corrective responses in visual probes by quantifying involuntary muscle responses in the SLR$_{visual}$ (90–120 ms) and LLR$_{visual}$ time windows (120–180 ms). The SLR$_{visual}$ is thought to involve subcortical feedback pathways, while the LLR$_{visual}$ has been linked to transcortical feedback circuits.[33,45–49] Figure 3C illustrates the responses of elbow flexor and extensor muscles during rightward cursor jumps. During the LLR$_{visual}$, participants increased the activity of the elbow flexor muscles ($\Delta\bar{x}$ = 0.06 nu, 95% CI

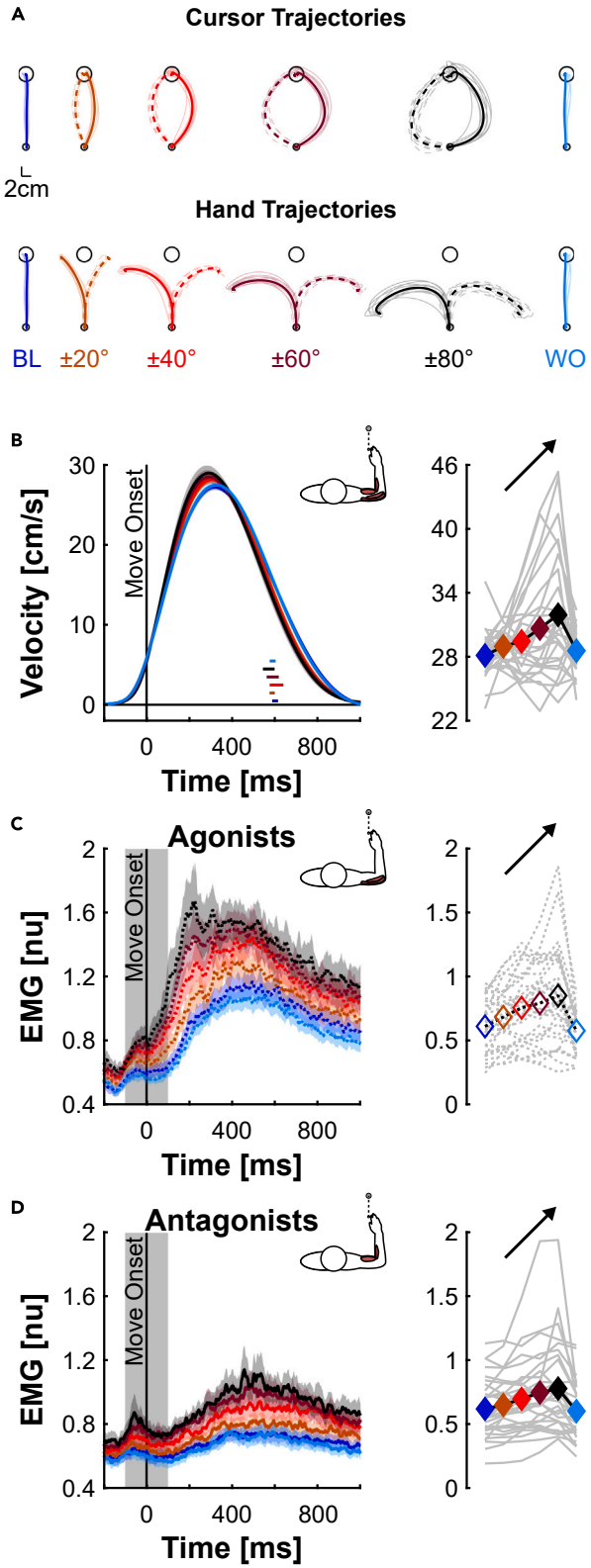
A
Cursor Trajectories
2cm
Hand Trajectories
BL
±20°
±40°
±60°
±80°
WO
B
Velocity [cm/s]
Move Onset
Time [ms]
C
Agonists
EMG [nu]
Move Onset
Time [ms]
D
Antagonists
EMG [nu]
Move Onset
Time [ms]

Figure 4. Properties of voluntary behavior and associated muscle activity of unperturbed trials in *Experiment 2*

(A) Exemplary cursor and hand trajectories performed by a representative participant in the absence (baseline and washout) or presence of unpredictable VMRs. Increasing the amplitude of the VMRs imposes larger cursor deviations and requires larger corrective responses to guide the feedback cursor into the goal target within the time constraints of the task.

(B) Group mean ± SE forward velocities in each phase of the experiment. The data are aligned with movement onset (t = 0 ms). Colored horizontal lines indicate the 95% confidence interval of the movement time across phases of the experiment. The side panel displays each individual's mean peak forward velocity (gray lines) and the corresponding group means (colored diamonds and black line) across experimental phases.

(C) Group mean ± SE activity of the elbow extensor muscles (solid lines) plotted in the same format as (B). The data were smoothed with a 10 sample (10 ms), zero-delay moving average for display purposes. The shaded, gray area (−100 to 100 ms) indicates the muscle activity associated with the planning and initiation of voluntary behavior. The side panel displays the average muscle activity surrounding movement onset.

(D) Group mean ± SE activity of the elbow flexor muscles (dashed lines) plotted in the same format as (C).

Arrows indicate statistically significant contrasts. BL, baseline; WO, washout; nu, normalized unit.

See also Figure S1.

[0.01, 0.10], t(29) = 2.51, $p = 0.018$, d = 0.6) and decreased the activity of the elbow extensor muscles ($\Delta\bar{x}$ = 0.12 nu, 95% CI [0.08, 0.16], t(29) = 6.15, $p < 0.001$, d = 0.9) in parallel with the variability of the VMRs. We did not observe statistically significant modulation of the SLR_{visual} (elbow flexors: $\Delta\bar{x}$ = 0.02 nu, 95% CI [−0.00, 0.04], t(29) = 1.75, $p = 0.091$, d = 0.2; elbow extensors: $\Delta\bar{x}$ = −0.00 nu, 95% CI [−0.05, 0.04], t(29) = −0.20, $p = 0.839$, d = −0.0). The findings suggest that the nervous system upregulates corrective responses through paired excitation of the agonists and inhibition of the antagonists in the long-latency time window.

In comparison to rightward cursor jumps, the modulation of responses to leftward cursor jumps (Figure 3D) occurred largely in the elbow extensor muscles (agonists). The elbow extensors were more active in the SLR_{visual} and LLR_{visual} time windows (SLR_{visual}: $\Delta\bar{x}$ = 0.08 nu, 95% CI [0.02, 0.15], t(29) = 2.83, $p = 0.008$, d = 0.6; LLR_{visual}: $\Delta\bar{x}$ = 0.17 nu, 95% CI [0.11, 0.23], t(29) = 5.84, $p < 0.001$, d = 1.0) when encountering more variable VMRs. The elbow flexor muscles (antagonists) did not display statistically significant modulation in either time window (SLR_{visual}: $\Delta\bar{x}$ = −0.02 nu, 95% CI [−0.07, 0.03], t(29) = −0.79, $p = 0.432$, d = −0.2; LLR_{visual}: $\Delta\bar{x}$ = −0.01 nu, 95% CI [−0.04, 0.02], t(29) = −0.87, $p = 0.393$, d = −0.1). Collectively, the results support the idea that the nervous system modulates its feedback gains in parallel to the variability of unpredictable visual disturbances.

The vigor of voluntary reaching movements, muscle coactivation, and responsiveness to visual feedback are tuned to increasingly variable visual disturbances

Experiment 1 demonstrated that the nervous system increases muscle coactivation and becomes more responsive to visual feedback when encountering more variable VMRs. The increase in feedback gains was evident in both the vigor of voluntary movements and corrective responses to the same visual probes. Motivated by these findings, we performed a second experiment to investigate the extent to which the nervous system upregulates coactivation and feedback gains when encountering increasingly variable VMRs (±20°, ±40°, ±60°, ±80°, Figures 4A and S1A). Increasing the amplitude of the VMRs imposes larger cursor deviations and requires larger corrective responses to guide the feedback cursor into the goal target within the time demands of the task.

Similar to *Experiment 1*, participants (N = 30) increased their peak forward hand velocities (Figure 4B, $\Delta\bar{x}$ = 2.8 cm/s, 95% CI [1.0, 4.7], t(29) = 3.17, $p = 0.004$, d = 0.8) during unperturbed trials. The largest peak forward velocities were evident when interacting with the most variable visuomotor rotations. In agreement with the results of *Experiment 1*, the modulation of peak forward velocities occurred in the absence of significant changes in movement times ($\Delta\bar{x}$ = 14 ms, 95% CI [−12, 39], t(29) = 1.07, $p = 0.292$, d = 0.2). In contrast to *Experiment 1*, we did not observe a graded shift of the peak forward velocity to earlier in movement across all experimental phases ($\Delta\bar{x}$ = −2 ms, 95% CI [−22, 18], t(29) = −0.20, $p = 0.841$, d = −0.0). However, a control analysis reproduced the results of *Experiment 1*. The peak velocities shifted to earlier in movement in the ±20° and ±40° VMR conditions relative to the baseline and washout phases ($\Delta\bar{x}$ = 16 ms, 95% CI [6, 27], t(29) = 3.25, $p = 0.003$, d = 0.4). Similar to *Experiment 1*, participants increased the activity of their elbow flexor (Figure 4C, $\Delta\bar{x}$ = 0.14 nu, 95% CI [0.07, 0.22], t(29) = 4.06, $p < 0.001$, d = 0.5) and extensor muscles (Figure 4D, $\Delta\bar{x}$ = 0.21 nu, 95% CI [0.13, 0.30], t(29) = 5.29, $p < 0.001$, d = 0.8) in unperturbed movements. Increases in muscle activity were most pronounced in the highest variability condition. Taken together, the results reveal an increase in feedback gains and muscle coactivation when encountering increasingly variable VMRs.

We also investigated changes in feedback gains by examining the lateral velocity of corrective responses in visual probe trials (Figures 5A and 5B). In line with *Experiment 1*, increases in the lateral velocities of the corrective responses paralleled the variability of the unpredictable VMRs. Larger lateral velocities were evident in the early (right: $\Delta\bar{x}$ = 2.3 cm/s, 95% CI [1.3, 3.3], t(29) = 4.60, $p < 0.001$, d = 1.1; left: $\Delta\bar{x}$ = 2.5 cm/s, 95% CI [1.6, 3.3], t(29) = 6.01, $p < 0.001$, d = 1.4) and late response windows (right: $\Delta\bar{x}$ = 6.1 cm/s, 95% CI [4.3, 7.9], t(29) = 6.85, $p < 0.001$, d = 1.8; left: $\Delta\bar{x}$ = 5.7 cm/s, 95% CI [4.2, 7.2], t(29) = 7.82, $p < 0.001$, d = 2.1) with the largest lateral velocities occurring in the condition with the most variable VMRs.

Finally, we examined rapid muscle responses in visual probe trials to gain insight into the neural implementation of the upregulated corrective responses. Following rightward visual probes (Figure 5C), participants increased the activity of the elbow flexor muscles and inhibition of the elbow extensor muscles in the LLR_{visual} time window. The responsiveness of the flexor and extensor muscles increased in parallel with the variability of the VMRs (elbow flexors: $\Delta\bar{x}$ = 0.12 nu, 95% CI [0.03, 0.22], t(29) = 2.71, $p = 0.011$, d = 0.7; elbow extensors: $\Delta\bar{x}$ = 0.29 nu, 95% CI [0.14, 0.44], t(29) = 3.91, $p < 0.001$, d = 1.0). Statistical differences were not present in the SLR_{visual} (elbow flexors: $\Delta\bar{x}$ = 0.01 nu, 95% CI [−0.01, 0.04], t(29) = 0.99, $p = 0.328$, d = 0.2; elbow extensors: $\Delta\bar{x}$ = 0.08 nu, 95% CI [−0.00, 0.16], t(29) = 1.93, $p = 0.064$, d = 0.4). Following leftward visual probes (Figure 5D), the elbow extensor muscles displayed increased excitation in the LLR_{visual} in parallel with the variability of the VMRs

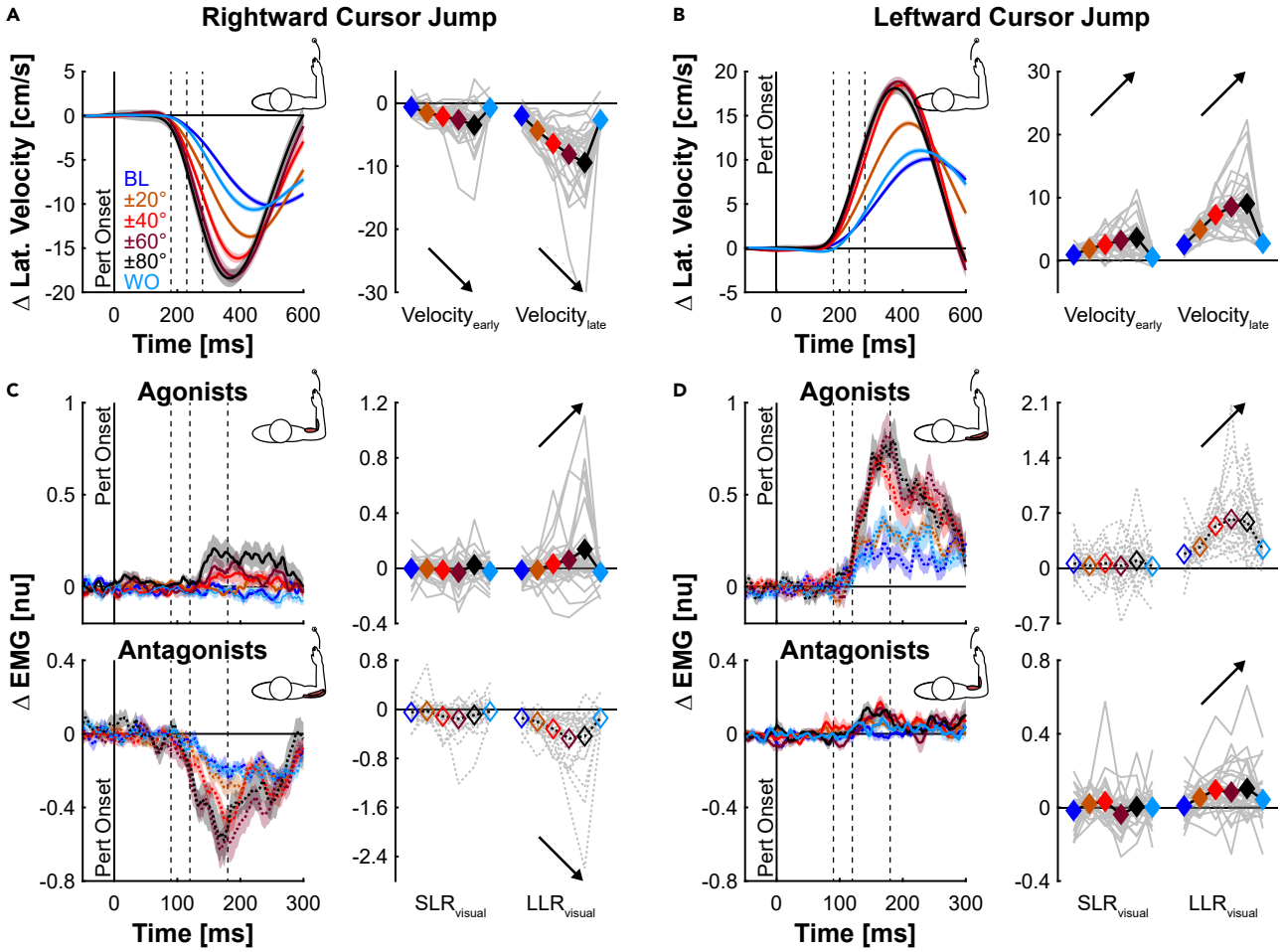

Figure 5. Lateral velocities and muscle responses during visual probes in *Experiment 2*

(A) Group mean ± SE change in lateral velocities in each phase of the experiment during rightward cursor jumps. The data are aligned with the onset of the visual probes (t = 0 ms). The dashed, vertical lines separate the velocity$_{early}$ (180–230 ms) and velocity$_{late}$ (230–280 ms) time windows. The side panel displays the mean lateral velocity in the velocity$_{early}$ and velocity$_{late}$ for each participant (gray lines) across experimental phases. The colored diamonds and black line represent the group means.

(B) Group mean ± SE change in lateral velocities in each phase of the experiment during leftward cursor jumps plotted in the same layout as (A).

(C) Group mean ± SE change in activity of the elbow flexor (solid lines, upper panel) and extensor muscles (dashed lines, lower panel) during rightward cursor jumps. The data are aligned with the onset of the visual probe (t = 0 ms). The dashed, vertical lines separate the SLR$_{visual}$ (90–120 ms) and LLR$_{visual}$ (120–180 ms). The data were smoothed with a 10 sample (10 ms), zero-delay moving average for display purposes. The side panels display the mean muscle activity in the SLR$_{visual}$ and LLR$_{visual}$ time windows for the elbow flexors (solid gray lines, upper panel) and extensors (dashed gray lines, lower panel) for each participant across experimental phases. The colored diamonds and black line represent the group means.

(D) Group mean ± SE change in activity of the elbow extensor (dashed lines, upper panel) and flexor muscles (solid lines, lower panel) during leftward cursor jumps plotted in the same format as (C).

Arrows indicate statistically significant contrasts. BL, baseline; WO, washout; nu, normalized unit.

($\Delta\bar{x}$ = 0.38 nu, 95% CI [0.26, 0.49], t(29) = 6.72, $p < 0.001$, d = 1.3), but not in the SLR$_{visual}$ time window ($\Delta\bar{x}$ = 0.03 nu, 95% CI [−0.04, 0.11], t(29) = 0.83, $p = 0.412$, d = 0.1). The elbow flexor muscles (antagonists) also displayed larger excitation during the LLR$_{visual}$ ($\Delta\bar{x}$ = −0.07 nu, 95% CI [−0.10, −0.03], t(29) = −3.51, $p = 0.001$, d = −0.6). Modulation of activity in the SLR$_{visual}$ time window was not statistically significant ($\Delta\bar{x}$ = 0.00 nu, 95% CI [−0.03, 0.04], t(29) = 0.21, $p = 0.834$, d = 0.0). In summary, the results support the idea that the nervous system modulates its feedback gains in parallel to the variability of the VMRs.

Exposure to unpredictable visual disturbances results in general upregulation of feedback responses

The results of *Experiments 1* and *2* show that the nervous system increases its feedback gains when encountering increasingly variable visual disturbances. *Experiment 3* examined whether the exposure to variable VMRs evoked a selective increase in responsiveness to visual feedback or a general upregulation of responses to visual and proprioceptive feedback. We reasoned that the mismatch between the cursor and

hand position may render proprioceptive feedback less reliable (cf.[50–53]) and result in a decrease in responsiveness to proprioceptive feedback. In contrast, the variability of the VMRs may elicit a general increase in feedback gains that upregulate the nervous system's responsiveness to both visual and proprioceptive feedback.[4,5]

We addressed this question in a third experiment. Similar to *Experiments 1* and *2*, participants performed goal-directed reaching movements in the absence or presence of unpredictable VMRs (Figures S1B and S2A). In addition to visual probes, we examined the responsiveness to proprioceptive feedback using mechanical perturbations that extended or flexed the elbow (±1.5 Nm).[12,13,28,46,54] Note that the hand feedback cursor was removed with the onset of the mechanical probes to ensure that corrective responses were based on limb afferent feedback.[51,55,56] Participants (N = 30) encountered VMRs with a single level of variability (±30°; see STAR Methods). If the nervous system selectively increases its responsiveness to visual feedback, we expect larger peak hand displacements and reduced muscle responses following mechanical probes. In contrast, if the nervous system generally increases its feedback gains, we expect reduced peak hand displacements and upregulated muscle responses following mechanical probes when encountering unpredictable visuomotor rotations.[4,5]

In agreement with *Experiments 1* and *2*, participants produced reaching movements with faster peak velocities and became more responsive to visual feedback when dealing with variable visual environments (Figures S2 and S3). Figures 6A and 6B illustrate the average lateral displacement of the hand when countering mechanical probes in different phases of the experiment. In agreement with a general upregulation in feedback gains, the peak lateral displacements were reduced in the exposure phase relative to baseline and washout (extension: $\Delta\bar{x}$ = 2.2 cm, 95% CI [1.7, 2.6], t(29) = 10.22, $p < 0.001$, d = 1.0; flexion: $\Delta\bar{x}$ = 1.4 cm, 95% CI [1.0, 1.8], t(29) = 7.16, $p < 0.001$, d = 0.9).

We then examined the activity of elbow flexor and extensor muscles following mechanical probes that extended the elbow (Figure 6C). Responses to proprioceptive feedback were extracted in the $SLR_{mechanical}$ (25–50 ms) and $LLR_{mechanical}$ (50–100 ms) time windows.[4,5,40,41] The $SLR_{mechanical}$ involves spinal feedback circuits, whereas the $LLR_{mechanical}$ includes transcortical feedback circuits.[12,13,28,54] Statistical modulation was not evident in the elbow flexors that were stretched by the mechanical probe ($SLR_{mechanical}$: $\Delta\bar{x}$ = 0.05 nu, 95% CI [−0.05, 0.14], t(29) = 0.99, p = 0.330, d = 0.2; $LLR_{mechanical}$: $\Delta\bar{x}$ = 0.32 nu, 95% CI [−0.07, 0.71], t(29) = 1.70, p = 0.100, d = 0.3). Instead, we found greater inhibitory responses of the elbow extensors (i.e., shortened muscles) in both the $SLR_{mechanical}$ ($\Delta\bar{x}$ = 0.17 nu, 95% CI [0.02, 0.32], t(29) = 2.29, p = 0.029, d = 0.6) and $LLR_{mechanical}$ ($\Delta\bar{x}$ = 0.25 nu, 95% CI [0.11, 0.39], t(29) = 3.53, p = 0.001, d = 0.9) when participants encountered variable VMRs in the exposure phase relative to baseline and washout. Following mechanical probes that flexed the elbow (Figure 6D), greater excitation of the elbow extensors (i.e., stretched muscles) was evident in the $LLR_{mechanical}$ ($\Delta\bar{x}$ = 0.57 nu, 95% CI [0.34, 0.80], t(29) = 5.02, $p < 0.001$, d = 0.6) but not in the $SLR_{mechanical}$ ($\Delta\bar{x}$ = 0.12 nu, 95% CI [−0.01, 0.26], t(29) = 1.83, p = 0.077, d = 0.5) in the exposure phase compared to baseline and washout. No statistical modulation was apparent in the elbow flexors ($SLR_{mechanical}$: $\Delta\bar{x}$ = −0.00 nu, 95% CI [−0.06, 0.06], t(29) = −0.01, p = 0.989, d = −0.0; $LLR_{mechanical}$: $\Delta\bar{x}$ = 0.01 nu, 95% CI [−0.10, 0.13], t(29) = 0.21, p = 0.834, d = 0.0). Taken together, the results support a general upregulation of feedback gains that increase the responsiveness to both visual and proprioceptive feedback.

Muscle coactivation and long-latency feedback responses predict larger behavioral responses to visual and proprioceptive feedback

The results in each experiment highlight increases in the coactivation of agonist and antagonist muscles and larger responses to sensory feedback when exposed to variable visuomotor rotations. Coactivation is often associated with changes in muscle stiffness that increase resistance against physical disturbances.[17,20–22] Changes in muscle coactivation are thought to occur in a feedforward manner that is independent from changes in the processing of sensory feedback for online control.[3,17,20–24] Recent work has questioned whether the nervous system may also leverage coactivation to alter its responsiveness to sensory feedback.[4,5,11,15,16]

We tested this idea by examining the relationship between the activity of agonist and antagonist muscles, surrounding movement onset, prior to any influences of neural feedback to the probes (BKG; see STAR Methods), and behavioral responses to the visual and mechanical probes using linear mixed effects models (Figure 7; Table S1). The findings generally supported the hypothesis that muscle coactivation is associated with higher gain responses to sensory feedback. We found that greater activity of the elbow extensor and flexor muscles was associated with a steeper slope of the velocity of corrections in visual probes (Figures 7A and 7B) and a reduction in peak hand displacement in mechanical probe trials (Figures 7C and 7D). Taken together, greater muscle coactivation correlated with faster and more vigorous responses to visual and proprioceptive feedback.

We also examined the relationship between long-latency muscle responses and the resulting behavioral corrections (Figures 7E–7H). We observed rich coordination of agonist and antagonist muscles that varied based on the direction and sensory modality of the perturbation. When the flexors were the agonist muscles for correcting visual probes, the responses were distributed such that both the flexor and extensor muscles contributed. Indeed, greater excitation of the elbow flexors and inhibition of the extensor muscles predicted faster responses to rightward cursor jumps (Figure 7E). In contrast, greater excitation of both elbow flexor (antagonist) and extensor (agonist) muscles predicted faster responses to leftward cursor jumps (Figure 7F). Responses to mechanical probes were mainly predicted by the agonist muscles. Indeed, greater excitation of the flexor muscles predicted reduced peak displacements during extension probes. Larger excitation of the extensor muscles predicted a reduction in peak displacements during flexion probes (Figure 7G&H). In summary, increased responsiveness to sensory feedback is linked with greater excitation of agonist, larger inhibition of antagonist muscles, or their shared responses during the long-latency time window.

DISCUSSION

Humans can encounter visual or physical disturbances when interacting with their environment. Here, we examined how the healthy nervous system alters the control of reaching movements when encountering VMRs that could change amplitude and direction between movements.

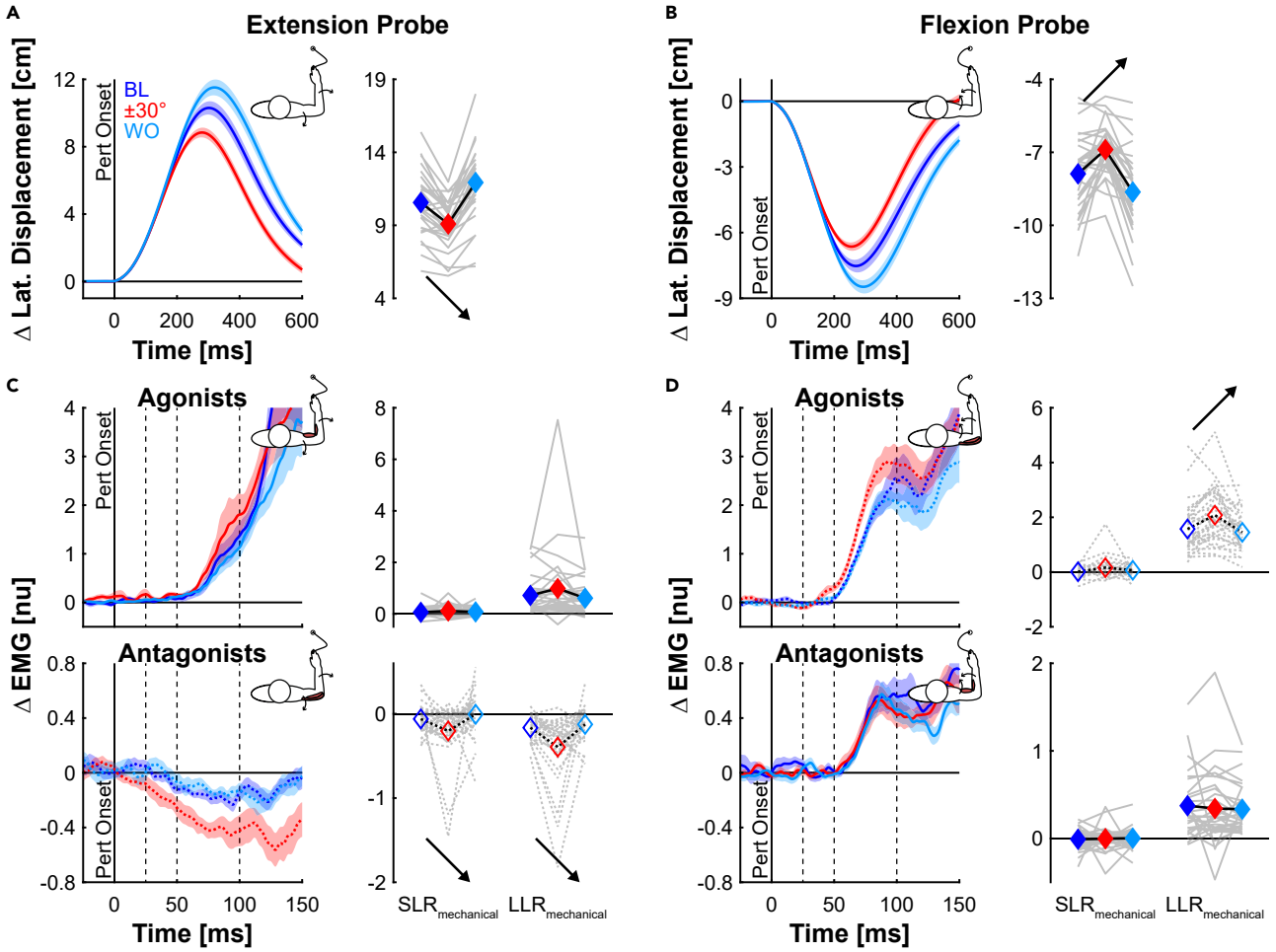

Figure 6. Lateral displacements and muscle responses during mechanical probes in *Experiment 3*

(A) Group mean ± SE change in lateral hand displacements in each phase of the experiment during extension probe trials. The data are aligned with the onset of the mechanical probes (t = 0 ms). The side panel displays the mean peak lateral hand displacement of each participant (gray lines) across experimental phases. The colored diamonds and black line represent the group means.

(B) Group mean ± SE change in lateral hand displacement in each phase of the experiment during flexion probe trials. The data are plotted in the same layout as (A).

(C) Group mean ± SE change in activity of the elbow flexor (solid lines, upper panel) and extensor muscles (dashed lines, lower panel) during extension probes. The data are aligned with the onset of the mechanical probes (t = 0 ms). The dashed, vertical lines separate the $SLR_{mechanical}$ (25–50 ms) and $LLR_{mechanical}$ (50–100 ms) time windows. The data were smoothed with a 10 sample (10 ms), zero-delay moving average for display purposes. The side panels display the mean muscle activity in the $SLR_{mechanical}$ and $LLR_{mechanical}$ time windows for the elbow flexors (solid gray lines, upper panel) and extensors (dashed gray lines, lower panel) for each participant across experimental phases. The colored diamonds and black lines represent the group means.

(D) Group mean ± SE change in activity of the elbow extensor (dashed lines, upper panel) and flexor muscles (solid lines, lower panel) during flexion probes plotted in the same format as (C).

Arrows indicate statistically significant contrasts. BL, baseline; WO, washout; nu, normalized unit.

See also Figures S1–S3.

We tested the hypothesis that the nervous system alters feedback gains when exposed to variable visual disturbances. Moreover, we examined whether muscle coactivation is associated with increased feedback gains and thus fast and vigorous responses to sensory feedback. When interacting with more variable visual disturbances, participants generated reaching movements with larger peak velocities, coactivated agonist and antagonist muscles, and became more responsive to visual and proprioceptive feedback. Across three experiments, upregulated behavioral responses to the same visual and mechanical disturbances were predicted by increases in muscle coactivation prior to the onset of perturbations. Behavioral responses were also predicted by the amplitude of long-latency responses of the agonist, antagonist, or both muscles. Collectively, the results demonstrate how the nervous system can exploit muscle coactivation to increase its responsiveness to sensory feedback when moving in unpredictable visual disturbances.

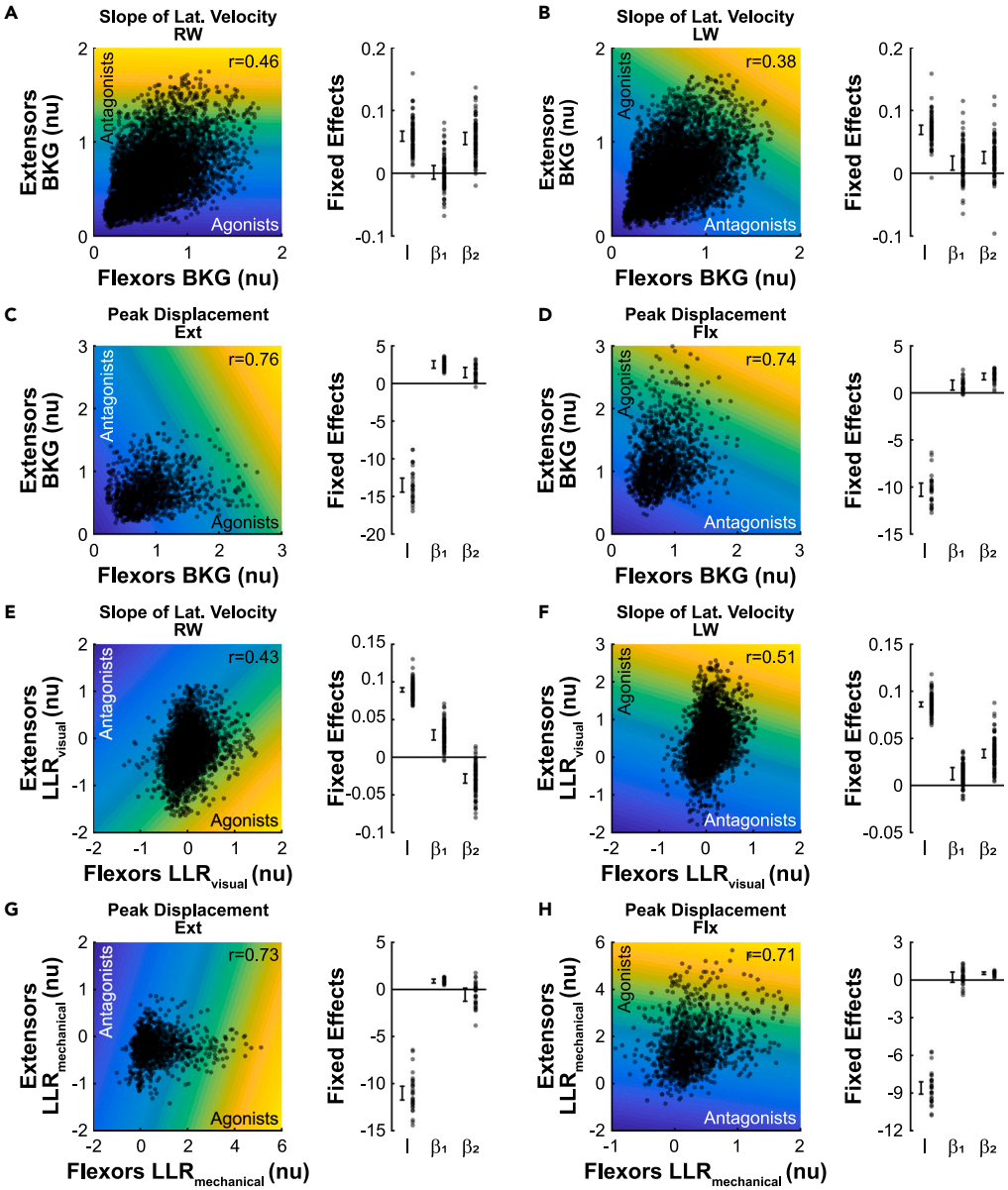

Figure 7. Relationship between muscle activity and responses to sensory feedback based on linear mixed effects models

(A) Relationship between the background muscle activity (BKG) of the elbow flexor and extensor muscles with the slope of the lateral velocity during rightward (RW) cursor jumps. Colored background indicates the planar fit of the model with brighter colors indicating a steeper slope of the lateral velocity. The side panel displays the 95% confidence intervals of the fixed effects of the model and each participant's individual intercept (I) and slopes (β_1: flexors; β_2: extensors).

(B) Relationship between BKG activity of the elbow flexor and extensor muscles and the slope of the lateral velocity during leftward (LW) cursor jumps. The data are plotted in the same layout as (A).

(C and D) Relationship between BKG of the elbow flexor and extensor muscles with the peak hand displacement during mechanical probes that caused extension (Ext) or flexion (Flx) of the elbow. The data are plotted in the same layout as (A) with brighter colors of the background indicating reduced peak hand displacements.

(E and F) Relationship between the LLR_{visual} of the elbow flexor and extensor muscles with the slope of the lateral velocity, plotted in the same layout as (A).

(G and H) Relationship between the $LLR_{mechanical}$ of the elbow flexor and extensor muscles with the peak hand displacement, plotted in the same layout as (C).

Agonist and antagonist muscles were defined relative to their action during the visual or mechanical probes.

See also Table S1.

We imposed visuomotor rotations that varied in direction and amplitude (present or absent) between trials. In each experiment, participants increased their peak movement velocities and became more responsive to the same visual and mechanical disturbances. The peak velocities also shifted to earlier in movement for less variable VMRs (i.e., $\leq \pm 40°$). For more variable VMRs, the timing of the peaks became

more variable across participants, making it difficult to detect subtle shifts in these peaks with the statistical analyses. The results compliment evidence that the nervous system increases feedback gains when exposed to mechanical disturbances that can vary in direction and amplitude.[4,5,14] Other studies have shown that the nervous system increases feedback gains when initially exposed to novel or unstable mechanical loads[1,2,25,57,58] as well as novel or variable visual disturbances.[34,59] The results collectively agree with the predictions of optimal feedback control theory. The theory offers a range of control strategies that differ in the assumptions they make about movement disturbances.[4,5,11,14] These assumptions in turn impact how efficient versus robust the control policy is to disturbances that arise during movement.[60] When faced with novel or variable disturbances, the best solution for maintaining task performance is to adopt the cautious but costly strategy of increasing feedback gains to make the control policy as robust to the disturbances as possible.[4,61,62] Taken together, our results suggest that the nervous system tolerates the cost of being more responsive to sensory feedback to mitigate errors that arise from variable disturbances.

Increased feedback gains in our experiments were accompanied by spontaneous increases in muscle coactivation. Muscle coactivation is traditionally thought to increase the stiffness of skeletal muscle to stabilize the arm and quickly resist physical disturbances.[17,20–22] Accordingly, the nervous system would have to trade off its stability for mobility by decreasing coactivation[63] to enable fast responses to the unpredictable visual disturbances. Contrary to this prediction, the participants in our experiment increased muscle coactivation in conditions where they also increased the mobility of their arm to quickly respond to the imposed visual errors. The changes in coactivation and responses to visual feedback call into question whether the sole purpose of muscle coactivation is to increase the stiffness of the arm to provide stability.

We argue that coactivation may help to increase the responsiveness of neural feedback loops to quickly mobilize the arm and correct for errors imposed by the variable rotations. The results align with the recent hypothesis that coactivation enables fast and vigorous responses to sensory feedback.[4,5,11,15,16] It is becoming clear that instructions to coactivate make the nervous system more responsive to mechanical perturbations while attempting to hold a fixed arm[16] or body posture.[15] When instructed to increase muscle coactivation, participants generated larger feedback responses, were displaced less when responding to the same physical perturbations, and returned faster to specific arm and body postures. In contrast to these studies, our experiments manipulated the amplitude of visual rotations to impose larger and more variable errors during movement. Participants were not explicitly instructed to coactivate their muscles but did so spontaneously. The levels of coactivation tended to be small, on average, but became more prominent when dealing with increasingly variable visual rotations. The increases in coactivation were associated with rich coordination and flexible muscle responses that engaged the agonist, antagonist, or both muscles for online control.

The findings reveal a link between muscle coactivation and the amplitude of muscle responses and the corrective responses to perturbations. On a trial-by-trial basis, increases in pre-perturbation activity of the agonist and antagonist muscles were associated with faster responses to visual disturbances and a reduction in the peak displacement of the arm in mechanical probe trials. The relationship between coactivation and corrective responses to sensory feedback contrasts with the idea that coactivation is set independently from online responses to sensory feedback.[18,20–24,58] Instead, this link suggests that the nervous system can leverage coactivation to increase mobility and enable fast behavioral responses to sensory feedback by facilitating rich, coordinated responses of the agonist, antagonist, or both muscles for control. Indeed, corrective responses were also predicted by the amplitude of long-latency responses of agonist and antagonist muscles.

There are several neural mechanisms that may allow the nervous system to leverage coactivation for fast and vigorous online control that accommodates properties of the task. Increases in the excitability of the spinal cord can enable faster net force output by altering motor unit (de)recruitment.[64,65] In turn, larger motor units can be poised above or near their recruitment threshold, thereby reducing the time required to produce larger responses to sensory feedback, both in terms of excitation and inhibition.[66] Increases in muscle coactivation can also lead to sharing of corrective responses across muscles.[15,16] Indeed, distributed responses to mechanical perturbations can increase the net torque output by leveraging excitation of the agonist, inhibition of the antagonist, or distributed responses that rely on reciprocal inhibition.[15] Such patterns of reciprocal inhibition are fundamental in allowing animals and insects to produce rapid actions through coactivation.[67,68] When responses were shared across muscles in our experiments (Figure 7E), the excitation of the agonistic flexors was relatively small (positive β-weight), but when paired with the inhibition of the antagonistic extensor muscles (negative β-weight), produced pronounced changes in behavioral responses to the perturbations. However, there are instances where some participants also increased the excitation of both the agonist and antagonist muscles during corrective responses (both positive β-weights; Figures 7E–7H). This finding highlights a range of muscle responses that can increase responsiveness to sensory feedback and that the nervous system does not simply rely on reciprocal inhibition of the agonist and antagonist muscles. Instead, our findings suggest that the nervous system may rely on the agonist muscles to increase feedback gains with the antagonist muscles serving to brake the corrective response (both positive β-weights), rely on the inhibition of the antagonist muscles (negative β-weight), or share the responses between the agonist and antagonist muscles. Finally, increases in coactivation can potentiate responses of muscle spindles[69–72] and upregulate responses to mechanical perturbations.[73] This mechanism may relate to the observation that increases in muscle activity alter the processing of proprioceptive signals in the primary somatosensory cortex during voluntary contractions.[74] Future studies are needed to understand how these mechanisms and their potential interplay enable flexible feedback control.

Muscle coactivation may prime spinal, subcortical, and cortical feedback circuits when the task requires high gain control in the healthy nervous system. This priming may arise from neural state changes that accompany coactivation (cf.[75]) or specific neural populations responsible for coactivation,[76,77] such that distributed neural circuits in the primary motor cortex,[75,78–80] cerebellum,[78,81,82] reticular formation,[76,79] and spinal cord[77] may become more responsive to sensory feedback. These areas contribute to the processing of sensory feedback of cortical, subcortical, and spinal circuits.[12,13,28,46,47,54,83,84] In some conditions, larger muscle responses were not

only evident in long-latency responses that involve cortical feedback circuits but also short-latency responses that implicate subcortical and spinal processing of visual and afferent feedback.[12,28,45,46,48,49] This raises a question of whether there are scenarios in which co-activation can shift the flexible control of sensory feedback from fast, cortical feedback loops to even faster, subcortical (visual) and spinal (proprioceptive) feedback circuits.

Our results raise additional questions about situations in which coactivation may facilitate goal-directed control or even detract from it in neurological conditions. Coactivation may also arise in other tasks that require high gain control, such as reaching to small targets in the presence of mechanical perturbations,[85] with increased timing demands,[38] or during whole-body postural control in threatening situations.[86,87] Coactivation is also prominent in many neurological diseases, such as stroke[88–91] or cerebral palsy,[92] where excessive coactivation may lead to upregulated and aberrant responses to sensory feedback. Future work is required to understand the importance of coactivation in producing fast and goal-directed responses to sensory feedback in health and neurological disease.

Limitations of the study

In this study, we exposed healthy human participants to unpredictable visual disturbances that could change in direction and amplitude (absence and presence) between trials. Participants were not instructed to coactivate their muscles. Instead, muscle coactivation emerged spontaneously and increased in parallel with responses to sensory feedback. Using this approach, we demonstrated that increased muscle coactivation was associated with larger responses to both visual and proprioceptive feedback, highlighting a link between muscle coactivation and responses to sensory feedback (cf.[18,20,21,23,24]). Our findings support the idea that muscle coactivation may prime the nervous system for fast and vigorous responses to sensory feedback when required by the task. The analyses also agree with recent work demonstrating that instructions to coactivate their muscles enable participants to generate larger responses to mechanical disturbances applied to the upper limb or in standing balance.[15,16] Additional work is needed to assess the causal role of muscle coactivation in increasing responses to visual feedback.

RESOURCE AVAILABILITY

Lead contact

Further information and requests for resources should be directed to and will be fulfilled by the lead contact, Tyler Cluff (tyler.cluff@ucalgary.ca).

Materials availability

This study did not generate new unique reagents.

Data and code availability

- All data reported in this paper will be shared by the lead contact upon request.
- This paper does not report original code. We used MATLAB (R2020b) and RStudio (1.1.463) to analyze the data in line with past research.
- Any additional information required to reanalyze the data reported in this paper is available from the lead contact upon request.

ACKNOWLEDGMENTS

This work was supported by the Natural Sciences and Engineering Research Council of Canada (NSERC) Discovery Grant (2017-04829) and startup funds from the Faculty of Kinesiology – University of Calgary and the Calgary Health Trust awarded to T.C. P.M. was supported by the Eyes High Doctoral Recruitment Scholarship from the University of Calgary. G.M. was supported by an NSERC Undergraduate Student Research Award. We would like to thank Jeremy Wong, Ryan Peters, and Walter Herzog for feedback on an earlier version of the manuscript.

AUTHOR CONTRIBUTIONS

Conceptualization, P.M., G.M., and T.C.; methodology, P.M., G.M., and T.C.; software, P.M., G.M., and T.C.; formal analysis, P.M. and T.C.; investigation, P.M. and G.M.; writing – original draft, P.M.; writing – review and editing, P.M., G.M., and T.C.; funding acquisition, T.C.; supervision, T.C.

DECLARATION OF INTERESTS

The authors declare no competing interests.

STAR★METHODS

Detailed methods are provided in the online version of this paper and include the following:

- Electromyography (EMG) recordings and analyses
- Statistical analyses

SUPPLEMENTAL INFORMATION

Supplemental information can be found online at https://doi.org/10.1016/j.isci.2024.111174.

Received: January 16, 2024
Revised: March 12, 2024
Accepted: October 10, 2024
Published: October 16, 2024

REFERENCES

1. Franklin, S., Wolpert, D.M., and Franklin, D.W. (2012). Visuomotor feedback gains upregulate during the learning of novel dynamics. J. Neurophysiol. *108*, 467–478.
2. Franklin, S., and Franklin, D.W. (2021). Feedback Gains modulate with Motor Memory Uncertainty. Neuron. Behav. Data Anal. Theory *5*, 1–28. https://doi.org/10.51628/001c.22336.
3. Franklin, D.W., Burdet, E., Osu, R., Kawato, M., and Milner, T.E. (2003). Functional significance of stiffness in adaptation of multijoint arm movements to stable and unstable dynamics. Exp. Brain Res. *151*, 145–157.
4. Crevecoeur, F., Scott, S.H., and Cluff, T. (2019). Robust Control in Human Reaching Movements: A Model-Free Strategy to Compensate for Unpredictable Disturbances. J. Neurosci. *39*, 8135–8148.
5. Maurus, P., Jackson, K., Cashaback, J.G.A., and Cluff, T. (2023). The nervous system tunes sensorimotor gains when reaching in variable mechanical environments. iScience *26*, 106756.
6. Izawa, J., Rane, T., Donchin, O., and Shadmehr, R. (2008). Motor Adaptation as a Process of Reoptimization. J. Neurosci. *28*, 2883–2891.
7. Hadjiosif, A.M., and Smith, M.A. (2015). Flexible Control of Safety Margins for Action Based on Environmental Variability. J. Neurosci. *35*, 9106–9121.
8. Gonzalez Castro, L.N., Hadjiosif, A.M., Hemphill, M.A., and Smith, M.A. (2014). Environmental consistency determines the rate of motor adaptation. Curr. Biol. *24*, 1050–1061.
9. Todorov, E., and Jordan, M.I. (2002). Optimal feedback control as a theory of motor coordination. Nat. Neurosci. *5*, 1226–1235.
10. Scott, S.H. (2004). Optimal feedback control and the neural basis of volitional motor control. Nat. Rev. Neurosci. *5*, 532–546.
11. Kalidindi, H.T., and Crevecoeur, F. (2023). Human reaching control in dynamic environments. Curr. Opin. Neurobiol. *83*, 102810.
12. Scott, S.H. (2012). The computational and neural basis of voluntary motor control and planning. Trends Cognit. Sci. *16*, 541–549.
13. Pruszynski, J.A., and Scott, S.H. (2012). Optimal feedback control and the long-latency stretch response. Exp. Brain Res. *218*, 341–359.
14. Córdova Bulens, D., Cluff, T., Blondeau, L., Moore, R.T., Lefèvre, P., and Crevecoeur, F. (2023). Different Control Strategies Drive Interlimb Differences in Performance and Adaptation during Reaching Movements in Novel Dynamics. eNeuro *10*, 1–13.
15. Martino, G., Beck, O.N., and Ting, L.H. (2023). Voluntary muscle coactivation in quiet standing elicits reciprocal rather than coactive agonist-antagonist control of reactive balance. J. Neurophysiol. *129*, 1378–1388.
16. Saliba, C.M., Rainbow, M.J., Selbie, W.S., Deluzio, K.J., and Scott, S.H. (2020). Co-contraction uses dual control of agonist-antagonist muscles to improve motor performance. Preprint at bioRxiv *1*, 1–42. https://doi.org/10.1101/2020.03.16.993527.
17. Burdet, E., Osu, R., Franklin, D.W., Milner, T.E., and Kawato, M. (2001). The central nervous system stabilizes unstable dynamics by learning optimal impedance. Nature *414*, 446–449.
18. Franklin, D.W., Liaw, G., Milner, T.E., Osu, R., Burdet, E., and Kawato, M. (2007). Endpoint Stiffness of the Arm Is Directionally Tuned to Instability in the Environment. J. Neurosci. *27*, 7705–7716.
19. Franklin, D.W., So, U., Kawato, M., and Milner, T.E. (2004). Impedance Control Balances Stability With Metabolically Costly Muscle Activation. J. Neurophysiol. *92*, 3097–3105.
20. Franklin, D.W., and Wolpert, D.M. (2011). Computational mechanisms of sensorimotor control. Neuron *72*, 425–442.
21. Hogan, N. (1984). Adaptive Control of Mechanical Impedance by Coactivation of Antagonist Muscles. IEEE Trans. Automat. Control *29*, 681–690.
22. Hogan, N. (1985). The mechanics of multi-joint posture and movement control. Biol. Cybern. *52*, 315–331.
23. Van Wouwe, T., Ting, L.H., and De Groote, F. (2022). An approximate stochastic optimal control framework to simulate nonlinear neuro-musculoskeletal models in the presence of noise. PLoS Comput. Biol. *18*, e1009338.
24. Berret, B., and Jean, F. (2020). Stochastic optimal open-loop control as a theory of force and impedance planning via muscle co-contraction. PLoS Comput. Biol. *16*, e1007414.
25. Calalo, J.A., Roth, A.M., Lokesh, R., Sullivan, S.R., Wong, J.D., Semrau, J.A., and Cashaback, J.G.A. (2023). The Sensorimotor System Modulates Muscular Co-Contraction Relative to Visuomotor Feedback Responses to Regulate Movement Variability. J. Neurophysiol. *129*, 751–766.
26. Crevecoeur, F., and Scott, S.H. (2014). Beyond Muscles Stiffness: Importance of State-Estimation to Account for Very Fast Motor Corrections. PLoS Comput. Biol. *10*, e1003869.
27. Burdet, E., Osu, R., Franklin, D.W., Yoshioka, T., Milner, T.E., and Kawato, M. (2000). A method for measuring endpoint stiffness during multi-joint arm movements. J. Biomech. *33*, 1705–1709.
28. Scott, S.H. (2016). A Functional Taxonomy of Bottom-Up Sensory Feedback Processing for Motor Actions. Trends Neurosci. *39*, 512–526.
29. Paz, R., Boraud, T., Natan, C., Bergman, H., and Vaadia, E. (2003). Preparatory activity in motor cortex reflects learning of local visuomotor skills. Nat. Neurosci. *6*, 882–890.
30. Huang, H.J., and Ahmed, A.A. (2014). Reductions in muscle coactivation and metabolic cost during visuomotor adaptation. J. Neurophysiol. *112*, 2264–2274.
31. Scott, S.H. (1999). Apparatus for measuring and perturbing shoulder and elbow. J. Neurosci. Methods *89*, 119–127.
32. Singh, K., and Scott, S.H. (2003). A motor learning strategy reflects neural circuitry for limb control. Nat. Neurosci. *6*, 399–403.
33. Cross, K.P., Cluff, T., Takei, T., and Scott, S.H. (2019). Visual feedback processing of the limb involves two distinct phases. J. Neurosci. *39*, 6751–6765.
34. Franklin, D.W., and Wolpert, D.M. (2008). Specificity of reflex adaptation for task-relevant variability. J. Neurosci. *28*, 14165–14175.
35. Furr, R.M., and Rosenthal, R. (2003). Evaluating theories efficiently: Nuts and bolts of contrast analysis. Underst. Stat. Stat. Issues Psychol. Educ. Soc. Sci. *2*, 45–67.
36. Rosenthal, R., and Rosnow, R.L. (1985). Contrast Analysis: Focused Comparisons in the Analysis of Variance (Cambridge University Press).
37. Rosenthal, R., Rosnow, R.L., and Rubin, D.B. (2000). Contrasts and Effect Sizes in Behavioral Research: A Correlational Approach (Cambridge University Press).
38. Poscente, S.V., Peters, R.M., Cashaback, J.G.A., and Cluff, T. (2021). Rapid Feedback Responses Parallel the Urgency of Voluntary Reaching Movements. Neuroscience *475*, 163–184. https://doi.org/10.1016/j.neuroscience.2021.07.014.
39. Debicki, D.B., and Gribble, P.L. (2005). Persistence of inter-joint coupling during single-joint elbow flexions after shoulder fixation. Exp. Brain Res. *163*, 252–257.
40. Maeda, R.S., Cluff, T., Gribble, P.L., and Pruszynski, J.A. (2018). Feedforward and Feedback Control Share an Internal Model of the Arm's Dynamics. J. Neurosci. *38*, 10505–10514.

41. Maeda, R.S., Gribble, P.L., and Pruszynski, J.A. (2020). Learning New Feedforward Motor Commands Based on Feedback Responses. Curr. Biol. *30*, 1941–1948.e3.
42. Maeda, R.S., Cluff, T., Gribble, P.L., and Pruszynski, J.A. (2017). Compensating for intersegmental dynamics across the shoulder, elbow, and wrist joints during feedforward and feedback control. J. Neurophysiol. *118*, 1984–1997.
43. Gribble, P.L., Mullin, L.I., Cothros, N., and Mattar, A. (2003). Role of Cocontraction in Arm Movement Accuracy. J. Neurophysiol. *89*, 2396–2405.
44. Heald, J.B., Franklin, D.W., and Wolpert, D.M. (2018). Increasing muscle co-contraction speeds up internal model acquisition during dynamic motor learning. Sci. Rep. *8*, 16355.
45. Georgopoulos, A.P., Kalaska, J.F., Caminiti, R., and Massey, J.T. (1983). Interruption of Motor Cortical Discharge Subserving Aimed Arm Movements. Exp. Brain Res. *49*, 327–340.
46. Cluff, T., Crevecoeur, F., and Scott, S.H. (2015). A perspective on multisensory integration and rapid perturbation responses. Vis. Res. *110*, 215–222.
47. Corneil, B.D., and Munoz, D.P. (2014). Overt responses during covert orienting. Neuron *82*, 1230–1243.
48. Gu, C., Wood, D.K., Gribble, P.L., and Corneil, B.D. (2016). A trial-by-trial window into sensorimotor transformations in the human motor periphery. J. Neurosci. *36*, 8273–8282.
49. Kozak, R.A., and Corneil, B.D. (2021). High-contrast, moving targets in an emerging target paradigm promote fast visuomotor responses during visually guided reaching. J. Neurophysiol. *126*, 68–81.
50. Crevecoeur, F., Munoz, D.P., and Scott, S.H. (2016). Dynamic Multisensory Integration: Somatosensory Speed Trumps Visual Accuracy during Feedback Control. J. Neurosci. *36*, 8598–8611.
51. Kasuga, S., Crevecoeur, F., Cross, K.P., Balalaie, P., and Scott, S.H. (2022). Integration of proprioceptive and visual feedback during online control of reaching. J. Neurophysiol. *127*, 354–372.
52. Ernst, M.O., and Banks, M.S. (2002). Humans integrate visual and haptic information in a statistically optimal fashion. Nature *415*, 429–433.
53. van Beers, R.J., Sittig, A.C., and Gon, J.J. (1999). Integration of Proprioceptive and Visual Position-Information: An Experimentally Supported Model. J. Neurophysiol. *81*, 1355–1364.
54. Scott, S.H., Cluff, T., Lowrey, C.R., and Takei, T. (2015). Feedback control during voluntary motor actions. Curr. Opin. Neurobiol. *33*, 85–94.
55. Kurtzer, I.L., Pruszynski, J.A., and Scott, S.H. (2008). Long-Latency Reflexes of the Human Arm Reflect an Internal Model of Limb Dynamics. Curr. Biol. *18*, 449–453.
56. Maurus, P., Kurtzer, I., Antonawich, R., and Cluff, T. (2021). Similar stretch reflexes and behavioral patterns are expressed by the dominant and nondominant arms during postural control. J. Neurophysiol. *126*, 743–762.
57. Franklin, S., Wolpert, D.M., and Franklin, D.W. (2017). Rapid visuomotor feedback gains are tuned to the task dynamics. J. Neurophysiol. *118*, 2711–2726.
58. Franklin, S., and Franklin, D.W. (2023). Visuomotor feedback tuning in the absence of visual error information. In Neuron. Behav. Data Anal. Theory, pp. 1–31.
59. Dimitriou, M. (2018). Task-dependent modulation of spinal and transcortical stretch reflexes linked to motor learning rate. Behav. Neurosci. *132*, 194–209.
60. Basar, T., and Bernhard, P. (1995). Hoo-optimal Control and Related Minimax Design Problems: A Dynamic Game Approach (Springer (Modern Birkhauser Classics)).
61. Ueyama, Y. (2014). Mini-max feedback control as a computational theory of sensorimotor control in the presence of structural uncertainty. Front. Comput. Neurosci. *8*, 1–14.
62. Bian, T., Wolpert, D.M., and Jiang, Z.P. (2020). Model-free robust optimal feedback mechanisms of biological motor control. Neural Comput. *32*, 562–595.
63. Huang, H.J., and Ahmed, A.A. (2011). Tradeoff between stability and maneuverability during whole-body movements. PLoS One *6*, e21815.
64. Henneman, E. (1957). Relation between size of neurons and their susceptibility to discharge. Science *126*, 1345–1347.
65. Henneman, E., Somjen, G., and Carpenter, D.O. (1965). Functional significance of cell size in spinal motoneurons. J. Neurophysiol. *28*, 560–580.
66. Heckman, C.J., and Enoka, R.M. (2012). Motor unit. Compr. Physiol. *2*, 2629–2682.
67. Ilton, M., Bhamla, M.S., Ma, X., Cox, S.M., Fitchett, L.L., Kim, Y., Koh, J.S., Krishnamurthy, D., Kuo, C.Y., Temel, F.Z., et al. (2018). The principles of cascading power limits in small, fast biological and engineered systems. Science *360*, eaao1082.
68. Kagaya, K., and Patek, S.N. (2016). Feed-forward motor control of ultrafast, ballistic movements. J. Exp. Biol. *219*, 319–333.
69. Kakuda, N., Vallbo, Å.B., and Wessberg, J. (1996). Fusimotor and skeletomotor activities are increased with precision finger movement in man. J. Physiol. *492*, 921–929.
70. Kakuda, N., Miwa, T., and Nagaoka, M. (1998). Coupling between single muscle spindle afferent and EMG in human wrist extensor muscles: Physiological evidence of skeletofusimotor (beta) innervation. Electroencephalogr. Clin. Neurophysiol. *109*, 360–363.
71. Vallbo, Å.B. (1974). Human Muscle Spindle Discharge during Isometric Voluntary Contractions. Amplitude Relations between Spindle Frequency and Torque. Acta Physiol. Scand. *90*, 319–336.
72. Dimitriou, M. (2014). Human muscle spindle sensitivity reflects the balance of activity between antagonistic muscles. J. Neurosci. *34*, 13644–13655.
73. Dimitriou, M. (2022). Human muscle spindles are wired to function as controllable signal-processing devices. Elife *11*, 1–14.
74. Giangrande, A., Cerone, G.L., Botter, A., and Piitulainen, H. (2024). Volitional muscle activation intensifies neuronal processing of proprioceptive afference in the primary sensorimotor cortex: an EEG study. J. Neurophysiol. *131*, 28–37. https://doi.org/10.1152/jn.00340.2023.
75. Warriner, C.L., Fageiry, S., Saxena, S., Costa, R.M., and Miri, A. (2022). Motor cortical influence relies on task-specific activity covariation. Cell Rep. *40*, 111427.
76. Murray, A.J., Croce, K., Belton, T., Akay, T., and Jessell, T.M. (2018). Balance Control Mediated by Vestibular Circuits Directing Limb Extension or Antagonist Muscle Co-activation. Cell Rep. *22*, 1325–1338.
77. Ronzano, R., Lancelin, C., Bhumbra, G.S., Brownstone, R.M., and Beato, M. (2021). Proximal and distal spinal neurons innervating multiple synergist and antagonist motor pools. Elife *10*, e70858.
78. Babadi, S., Vahdat, S., and Milner, T.E. (2021). Neural substrates of muscle co-contraction during dynamic motor adaptation. J. Neurosci. *41*, 5667–5676.
79. Glover, I.S., and Baker, S.N. (2022). Both Corticospinal and Reticulospinal Tracts Control Force of Contraction. J. Neurosci. *42*, 3150–3164.
80. Humphrey, D.R., and Reed, D.J. (1983). Separate cortical systems for control of joint movement and joint stiffness: reciprocal activation and coactivation of antagonist muscles. Adv. Neurol. *39*, 347–372.
81. Frysinger, R.C., Bourbonnais, D., Kalaska, J.F., and Smith, A.M. (1984). Cerebellar cortical activity during antagonist cocontraction and reciprocal inhibition of forearm muscles. J. Neurophysiol. *51*, 32–49.
82. Wetts, R., Kalaska, J.F., and Smith, A.M. (1985). Cerebellar nuclear cell activity during antagonist cocontraction and reciprocal inhibition of forearm muscles. J. Neurophysiol. *54*, 231–244.
83. Kurtzer, I.L. (2015). Long-latency reflexes account for limb biomechanics through several supraspinal pathways. Front. Integr. Neurosci. *8*, 1–19.
84. Zonnino, A., Farrens, A.J., Ress, D., and Sergi, F. (2021). Measurement of stretch-evoked brainstem function using fMRI. Sci. Rep. *11*, 12544–12621.
85. Cross, K.P., Guang, H., and Scott, S.H. (2023). Proprioceptive and Visual Feedback Responses in Macaques Exploit Goal Redundancy. J. Neurosci. *43*, 787–802.
86. Horslen, B.C., Zaback, M., Inglis, J.T., Blouin, J.S., and Carpenter, M.G. (2018). Increased human stretch reflex dynamic sensitivity with height-induced postural threat. J. Physiol. *596*, 5251–5265.
87. Zaback, M., Adkin, A.L., and Carpenter, M.G. (2019). Adaptation of emotional state and standing balance parameters following repeated exposure to height-induced postural threat. Sci. Rep. *9*, 12449–12512.
88. Song, R., and Tong, K.Y. (2013). Myoelectrically controlled wrist robot for stroke rehabilitation. J. NeuroEng. Rehabil. *10*, 52.
89. Sheng, W., Li, S., Zhao, J., Wang, Y., Luo, Z., Lo, W.L.A., Ding, M., Wang, C., and Li, L. (2022). Upper Limbs Muscle Co-contraction Changes Correlated With the Impairment of the Corticospinal Tract in Stroke Survivors: Preliminary Evidence From Electromyography and Motor-Evoked Potential. Front. Neurosci. *16*, 886909–886913.
90. Hammond, M.C., Fitts, S.S., Kraft, G.H., Nutter, P.B., Trotter, M.J., and Robinson, L.M. (1988). Co-contraction in the hemiparetic forearm: Quantitative EMG evaluation. Arch. Phys. Med. Rehabil. *69*, 348–351.
91. Kamper, D.G., and Rymer, W.Z. (2001). Impairment of voluntary control of finger

motion following stroke: Role of inappropriate muscle coactivation. Muscle Nerve *24*, 673–681.

92. Poon, D.M.Y., and Hui-Chan, C.W.Y. (2009). Hyperactive stretch reflexes, co-contraction, and muscle weakness in children with cerebral palsy. Dev. Med. Child Neurol. *51*, 128–135.
93. Kurtzer, I., Pruszynski, J.A., and Scott, S.H. (2009). Long-Latency Responses During Reaching Account for the Mechanical Interaction Between the Shoulder and Elbow Joints. J. Neurophysiol. *102*, 3004–3015.
94. Kurtzer, I., Crevecoeur, F., and Scott, S.H. (2014). Fast feedback control involves two independent processes utilizing knowledge of limb dynamics. J. Neurophysiol. *111*, 1631–1645.
95. Krakauer, J.W., Ghilardi, M.-F., and Ghez, C. (1999). Independent learning of internal models for kinematic and dynamic control of reaching. Nature *2*, 1026–1031.
96. Fernandes, H.L., Stevenson, I.H., and Kording, K.P. (2012). Generalization of stochastic visuomotor rotations. PLoS One *7*, e43016.
97. Albert, S.T., Jang, J., Sheahan, H.R., Teunissen, L., Vandevoorde, K., Herzfeld, D.J., and Shadmehr, R. (2021). An implicit memory of errors limits human sensorimotor adaptation. Nat. Human Behav. *5*, 920–934.
98. Pruszynski, J.A., Kurtzer, I., and Scott, S.H. (2008). Rapid Motor Responses Are Appropriately Tuned to the Metrics of a Visuospatial Task. J. Neurophysiol. *100*, 224–238.
99. De Comite, A., Crevecoeur, F., and Lefèvre, P. (2022). Reward-Dependent Selection of Feedback Gains Impacts Rapid Motor Decisions. eNeuro *9*, 1–14.
100. Crevecoeur, F., Kurtzer, I., Bourke, T., and Scott, S.H. (2013). Feedback responses rapidly scale with the urgency to correct for external perturbations. J. Neurophysiol. *110*, 1323–1332.
101. Cluff, T., and Scott, S.H. (2013). Rapid Feedback Responses Correlate with Reach Adaptation and Properties of Novel Upper Limb Loads. J. Neurosci. *33*, 15903–15914.
102. Cluff, T., and Scott, S.H. (2015). Apparent and actual trajectory control depend on the behavioral context in upper limb motor tasks. J. Neurosci. *35*, 12465–12476.
103. Sainburg, R.L. (2016). Laterality of Basic Motor Control Mechanisms: Different Roles of the Right and Left Brain Hemispheres. In Laterality in Sports: Theories and Applications (Elsevier Inc), pp. 155–177. https://doi.org/10.1016/B978-0-12-801426-4.00008-0.
104. Lakens, D. (2013). Calculating and reporting effect sizes to facilitate cumulative science: A practical primer for t-tests and ANOVAs. Front. Psychol. *4*, 1–12.
105. Goulet-Pelletier, J.-C., and Cousineau, D. (2018). A review of effect sizes and their confidence intervals, Part I: The Cohen's d family. Quant. Method. Psychol. *14*, 242–265.
106. R Core Team (2022). R: A language and environment for statistical computing. https://www.r-project.org/.
107. Johnson, R.A., and Wicher, D.W. (2019). Applied Multivariate Statistical Analysis (Pearson Modern Classic).

STAR★METHODS

KEY RESOURCES TABLE

REAGENT or RESOURCE	SOURCE	IDENTIFIER
Software and algorithms		
MATLAB (R2020b)	MathWorks	RRID: SCR_001622
RStudio (1.1.463)	RStudio Inc.	RRID: SCR_000432
Other		
Kinarm exoskeleton	Kinarm	https://kinarm.com/
Delsys Bagnoli DE-2.1 EMG Sensors	Delsys	https://delsys.com/

EXPERIMENTAL MODEL AND STUDY PARTICIPANT DETAILS

A total of 90 adults participated in one of three experiments (45 males, 45 females, between 18 and 38 years of age, 3 left-handed individuals). Handedness was assessed based on participant self-report. Thirty individuals participated in *Experiment 1*, 30 in *Experiment 2*, and 30 in *Experiment 3*. We recruited an equal number of males and females in each experiment. The participants had normal or corrected-to-normal vision and no known neurological or musculoskeletal impairments. The protocols were approved by the Conjoint Health and Research Ethics Board at the University of Calgary and participants provided written consent prior to beginning the experiment (REB16-1670). Each experiment took between 120 and 150 min to complete including set up time. Participants received a payment of $20 CAD and were free to withdraw from the study at any time without penalty.

METHOD DETAILS

Apparatus

Participants performed goal-directed reaching movements while seated with their dominant arm supported by a robotic exoskeleton (Kinarm, Kingston, ON, Canada).[31,32] The robot can apply torques at the shoulder and/or elbow joint(s) while participants perform upper limb movements in a transverse plane. The robot is paired with an LCD monitor that projected virtual targets and a hand-aligned feedback cursor (white circle aligned with the tip of the index finger, 0.5 cm radius) into the participant's workspace via a semi-silvered mirror. The setup enables the presentation of visual stimuli while manipulating the position of the cursor relative to the true position of the participant's hand. Direct vision of the arm and hand were blocked by a metal shutter throughout the experiments.

General task description

Participants initiated each trial by moving their feedback cursor into a start position (0.65 cm radius) located at a shoulder angle of 0° (relative to the frontal plane) and an elbow angle of 90° (relative to the upper arm; Figure 1A). Following a random hold period (1000–1200 ms, uniform distribution), a goal target (1.5 cm radius) appeared 15 cm directly in front of the start position. Participants were instructed to move the feedback cursor into the goal target within 500–700 ms and remain in the target for 750 ms. Explicit timing feedback was provided while participants held their feedback cursor in the target at the end of each trial. Movement time was calculated from the instant the participant left the start position until they entered the goal target.[5,26,38,56] The target turned green and 'Good Timing' was displayed following successful trials. The target turned blue and 'Speed up' was displayed if movements were too slow (>700 ms) or turned red and 'Slow down' was displayed if movements were too fast (<500 ms). The goal target disappeared after a brief delay (1000 ms), and participants moved back to the start position to initiate the next trial.

Experiment 1

This experiment examined how the nervous system alters the control of reaching movements in unpredictable visual environments. Participants were exposed to unpredictable visuomotor rotations (VMRs) that altered the mapping between the position of their occluded hand and a virtual feedback cursor displayed in the workspace. The VMRs rotated the cursor position clockwise or counterclockwise relative to the hand position on randomly selected trials (Figures 1B–1D). Participants had to correct in the direction opposite to the rotation to move the cursor into the target and complete the trial. Due to the unpredictable trial-by-trial changes in the direction of the rotations, participants could not anticipate the visual disturbances and had to quickly mobilize their arm to complete a trial within the timing demands of the task.

We probed neural feedback gains by applying 'cursor jump' perturbations on randomly selected trials.[1,2,33,34] We refer to the cursor jumps as visual probes because they provide an assay of the feedback gains. During the visual probes, the participant's hand-aligned cursor jumped perpendicular to the reach direction (±4 cm) when the participant left the start position (Figures 1B–1D). Successful performance required that participants generate a corrective response in the opposite direction to move the cursor into the goal target within the allotted time

window. The cursor was briefly removed from the screen (500 ms) at the end of the trial and realigned with the true position of the participant's index fingertip.

The experiment was composed of baseline, exposure, and washout phases. During the baseline phase, participants reached to the goal target in the absence of unpredictable VMRs. We refer to these trials as unperturbed trials. Visual probes were applied on randomly selected trials throughout baseline. Participants performed 150 trials that were organized in blocks of 8 unperturbed trials and 2 visual probes (+4 cm and −4 cm). Participants then moved into the exposure phase, where they encountered unpredictable VMRs on randomly selected trials. The VMRs had one of two levels of variability in separate subphases of exposure (±20° or ±30°). Note the variability of the applied VMRs increases with their amplitude since they deviate more from the mean on any given trial (0°). The order of the conditions was counterbalanced such that 15 participants encountered the ±20° VMRs first and 15 encountered the ±30° VMRs first. Unperturbed trials were randomly interleaved throughout the exposure phase to quantify changes in the forward velocity of voluntary reaching movements.[4,5] Participants performed 300 trials in each part of the exposure phase. The trials were presented in blocks consisting of 3 clockwise VMRs, 3 counterclockwise VMRs, 2 unperturbed trials, and 2 visual probes (+4 cm and −4 cm). The unpredictable VMRs were removed in the washout phase, where participants performed 150 trials that were identical to baseline. Participants performed 100 practice trials to familiarize themselves with the testing conditions before they completed the main experiment. The protocol, timing demands, and proportion of visual probes were identical to the baseline phase of the experiment.

Experiment 2

We conducted a follow-up experiment to assess the extent to which individuals alter their behavior and muscle activity when interacting with increasingly variable visual environments. The design of *Experiment 2* was similar to *Experiment 1*. Here, the exposure phase was split into four subphases where participants encountered VMRs with four different levels of variability (Figure S1A). The VMRs rotated the cursor position by ±20°, ±40°, ±60°, and ±80° relative to the hand position. The unpredictable VMRs were applied on randomly selected trials. All participants encountered the VMRs in order from the lowest to the highest variability. This decision was justified given the lack of statistically significant order effects in *Experiment 1* (Table S2). Unperturbed trials were randomly interleaved throughout the exposure phase. In each subphase of the exposure phase, participants performed 150 trials that were presented in blocks of 3 clockwise VMRs, 3 counterclockwise VMRs, 2 unperturbed trials, and 2 visual probes (+4 cm and −4 cm). This helped to maintain the time to complete the experiment and mitigate potential effects of fatigue.

Experiment 3

We performed a third experiment to test whether exposure to variable visual disturbances results in a general upregulation in responsiveness to sensory feedback. In addition to the visual probes used in *Experiments 1* and *2*, we integrated mechanical perturbations to probe the responsiveness to proprioceptive feedback.[12,13,28,46,54] We refer to these trials as mechanical probes. The mechanical perturbations were applied at the onset of randomly selected reaching movements (±1.5 Nm at the shoulder and elbow joints, 10 ms sigmoidal ramp-up),[5] disturbed elbow motion, and displaced the hand predominantly perpendicular to the reach direction. Shoulder motion remained unaltered for >100 ms following perturbation onset.[55,93,94] Contrary to our previous work, the feedback cursor was removed with the onset of the perturbation and restored after 400 ms[5,38]. This procedure ensured that corrective responses reflected contributions from limb afferent feedback and could not be attributed to increased responsiveness to visual feedback during mechanical probes.[51,55,56] Participants were instructed to reach the goal target within the same time window as unperturbed trials. The mechanical probes were turned off slowly while timing feedback was displayed at the end of the trial (1000 ms sigmoidal ramp-down). We also randomly interleaved unperturbed trials during which the cursor feedback disappeared with the onset of movement and reappeared after 400 ms. These trials were used as a reference for the kinematics and muscle activity recorded during mechanical probes.

The main experiment included a baseline, exposure, and washout phase (Figure S1B). Participants performed 270 trials in baseline. The trials were presented in blocks of 12 unperturbed trials with visual feedback, 2 unperturbed trials without visual feedback, 2 visual probes (+4 cm and −4 cm), and 2 mechanical probes (+1.5 Nm and −1.5 Nm). In the exposure phase, participants encountered VMRs that rotated the cursor position in the counterclockwise or clockwise direction by 30°. We opted for one level of variability to simplify the experiment and chose this amplitude of cursor rotation since it has been used extensively in past studies.[30,95–97] Participants performed 270 trials in the exposure phase. The trials were presented in blocks of 6 clockwise VMRs, 6 counterclockwise VMRs, 1 unperturbed trial with cursor feedback, 1 unperturbed trial without cursor feedback, 2 visual probes (+4 cm and −4 cm), and 2 mechanical probes (+1.5 Nm and −1.5 Nm). Note that we increased the number of VMRs to offset the larger variability introduced by probing responses to both visual and proprioceptive feedback. After the exposure phase, participants performed another 270 trials during washout. The trials were divided into blocks that were identical to baseline. Before the main experiment, participants completed a brief familiarization task that consisted of 90 practice trials organized in blocks that were identical to baseline.

QUANTIFICATION AND STATISTICAL ANALYSIS

Kinematic recordings and analyses

Elbow and shoulder kinematics were recorded by the robotic device at 1000 Hz. Hand position data were calculated based on joint kinematics and the calibration of the robotic device. The kinematic data were filtered (low-pass, 2nd order, dual-pass Butterworth filter, 30 Hz cutoff)

before further analysis.[55,98] Unperturbed trials were aligned to movement onset, which was defined as the instant the participant's hand left the start target.[4,5] For movements of fixed duration, increased feedback gains will result in reaching movements with larger peak forward velocities.[4–6] Thus, the peak forward hand velocity was used as a proxy for the feedback gains underlying voluntary movements.[4,5,14,99] We also calculated the movement times of unperturbed trials.[5,38,100]

Lateral velocities were calculated for all visual probes across all experiments. The lateral velocity of unperturbed trials was subtracted from the lateral velocity recorded during the visual probes in each experimental phase.[5,33] We then quantified the feedback gains by averaging the lateral velocities in an early ($Velocity_{early}$: 180 to 230 ms) and late ($Velocity_{late}$: 230 to 280 ms) time window.[2,5,33,58] The data were aligned with the onset of the cursor jump. We accounted for the time delay introduced by the TV screen quantified using a photodiode.

In *Experiment 3*, we also examined the lateral hand displacements (i.e., perpendicular to a straight line between the start and goal targets) during mechanical probes. The peak lateral hand displacements were extracted after subtracting the lateral hand displacements of unperturbed trials without visual feedback (cf.[4,5,38,99]). The data were aligned with the onset of the torque perturbations. All outcome variables were extracted for each trial and condition before averaging them for each experimental phase and participant. The kinematic processing and analyses were performed in MATLAB (R2020b, MathWorks).

Electromyography (EMG) recordings and analyses

The activity of the brachioradialis, triceps lateralis, biceps brachii, and triceps longus muscles were recorded using surface electromyography (DE 2.1 Single Differential Electrode, Delsys, Boston, MA, USA). The recording sites were shaved to remove hair, if necessary, and the skin was cleaned with isopropyl alcohol. After coating the electrode with a conductive gel, we secured it to the skin overlaying the muscle belly in parallel with the direction of the muscle fibers. A ground electrode was placed on the lateral epicondyle of the dominant elbow. EMG signals were sampled at 1 kHz and amplified online (gain = 10^3-10^4). EMG data were band-pass filtered (3^{rd} order, dual-pass Butterworth filter, 20 and 450 Hz) and full-wave rectified before further analysis.[55,98] An EMG normalization task was performed prior to the experiments to normalize the activity of each muscle to the average activity required to counter known reference loads (1 Nm extension or flexion torque at the elbow).[101,102] The EMG normalization task was performed in the same start position as the main experiments and consisted of five 15-s trials for each torque direction.[101,102]

We examined the averaged background muscle activity surrounding movement onset (BKG: −100 to 100 ms).[5,39–43] Note that we simplified the EMG analysis by averaging the activity of the elbow flexor (brachioradialis & biceps brachii) and extensor (triceps lateralis & triceps longus) muscles as similar responses were observed across synergistic muscles throughout the experiment.[5,44]

Across all experiments, we examined visual feedback gains using the muscle activity recorded in visual probes. The EMG activity in unperturbed trials with cursor feedback was subtracted from the EMG activity observed during each visual probe.[33] Based on this ΔEMG, we quantified rapid responses to visual feedback by averaging the muscle activity in the short-latency response (SLR_{visual}: 90 to 120 ms) and long-latency response (LLR_{visual}: 120 to 180 ms) time windows.[2,5,33,58]

In *Experiment 3*, we also examined proprioceptive feedback gains using the muscle activity during mechanical probes. We subtracted the average EMG activity during unperturbed trials without cursor feedback from the EMG activity during mechanical probes.[5,38,93,101,102] Subsequently, responses to proprioceptive feedback were extracted in the $SLR_{mechanical}$ (25–50 ms) and $LLR_{mechanical}$ (50–100 ms) time windows.[4,5,40,41] These SLR and LLR time windows provide insight into the neural implementation of the corrective responses to sensory feedback. SLRs are used to examine contributions from spinal (mechanical probes) and subcortical (visual probes) feedback processing, whereas LLRs are used to understand transcortical feedback processing through the primary motor cortex.[12,13,28,45–49,54] The EMG data processing and analyses were performed in MATLAB (R2020b, MathWorks).

Statistical analyses

We pooled the data from left- and right-handed participants for the statistical analysis. This decision is justified since the experiments followed a within-subject design, such that any comparisons are performed against each participant's own data. Moreover, left- and right-handed participants should not be expected to show opposite patterns of motor behavior (cf.[103]). Outcome variables were compared across phases of each experiment (baseline, exposure, and washout) using contrast analyses. Contrast analyses are statistical procedures that examine a specific research question and have higher statistical power than omnibus repeated measures ANOVA.[35–37] The experimental phases (e.g., baseline, ±20° VMR, ±30° VMR, & washout) were represented using fixed weights (λ-weights) that reflect a specific trend (e.g., linear trend) with the sum of all weights equal to zero.[35–37] Note that we only included the last 33% of trials of the baseline and washout phases in the statistical analysis due to past evidence that feedback gains and muscle responses during reaching decrease over time and reach an asymptote in the baseline and washout phases.[1,30,34,40,41] We assessed all trials during the exposure phase.

Past work suggests that control strategies are tuned to the variability of disturbances.[5–8] Accordingly, we expected that the outcome measures would change in parallel with the variability of the VMRs relative to baseline and washout. We used extended linear trends in *Experiment 1* ($\lambda_{baseline} = -\frac{3}{6}$, $\lambda_{\pm 20^\circ} = \frac{1}{6}$, $\lambda_{\pm 30^\circ} = \frac{5}{6}$, $\lambda_{washout} = -\frac{3}{6}$) and *Experiment 2* ($\lambda_{baseline} = -\frac{5}{12}$, $\lambda_{\pm 20^\circ} = -\frac{2}{12}$, $\lambda_{\pm 40^\circ} = \frac{1}{12}$, $\lambda_{\pm 60^\circ} = \frac{4}{12}$, $\lambda_{\pm 80^\circ} = \frac{7}{12}$, $\lambda_{washout} = -\frac{5}{12}$). The models include a linear trend (cf.[35–37]) to reflect an increase in the outcome measure in parallel with the variability of the VMRs, with a return to baseline levels during washout. A quadratic trend was used in *Experiment 3* ($\lambda_{baseline} = -\frac{1}{2}$, $\lambda_{\pm 30^\circ} = 1$, $\lambda_{washout} = -\frac{1}{2}$).[35–37] The λ-weights indicate a predicted increase in the outcome variable. The signs were switched if we expected a decrease in the variable (e.g., increased inhibition of muscle responses). Therefore, positive effect sizes align with our experimental

predictions. The α-level threshold was set to 0.05. We calculated and reported the contrast scores ($\Delta\bar{x}$), the corresponding 95% confidence intervals (CI), t-statistics, *p*-values, and Cohen's d.[35–37] We calculated Cohen's d as follows (cf.[104,105]):

$$Cohen's\ d = \frac{\Delta\bar{x}}{SD_{av}}$$

$$SD_{av} = \sqrt{\frac{\sum SD_i^2}{N}}$$

$\Delta\bar{x}$ is the contrast score. SD_i is the standard deviation of each experimental phase. N is the total number of phases included in the contrast analysis for each experiment. The contrast analyses were performed in RStudio.[106] Statistically significant contrasts were highlighted with arrows in the figures.

Finally, we investigated the relationship between the muscle activity and the responsiveness to sensory feedback. We determined the activity of the elbow flexor and extensor muscles surrounding movement onset (BKG) or during the LLR_{visual} and the slope of the lateral velocities of the same visual probes for each trial and participant. Note that the BKG muscle activity during visual probes did not include any contributions from neural feedback. The BKG or $LLR_{mechanical}$ and their corresponding peak lateral hand displacement were also extracted during the same mechanical probes. During mechanical probes, we only extracted the BKG muscle activity until movement onset (−100 to 0 ms) to avoid contributions from proprioceptive feedback. We flipped the sign of the slopes of the lateral velocities during rightward cursor jumps and of the peak lateral hand displacement during extension probes to simplify the interpretation. Thus, a larger positive slope of the lateral velocity indicates an increase in responsiveness to visual feedback. Similarly, a reduction in peak hand displacement reflects an increase in responsiveness to proprioceptive feedback. We combined the data across experimental phases and each participant before removing multivariate outliers based on the generalized squared distances with $\alpha = 0.05$,[107] which resulted in an average of ~1 trial being removed for each direction of perturbation and phase of the experiment. Removing the multivariate outliers did not impact the conclusions of the findings. We then performed linear mixed effects models (LMEs) to examine the relationship between the BKG or LLRs of elbow flexor and extensor muscles and the behavioral response to sensory feedback. The LMEs included three fixed effects (I: intercept, β_1: elbow flexor activity, and β_2: elbow extensor activity) with random intercept and slope for each participant using maximum likelihood estimation. We reported the average and 95% CI of the fixed effects with their corresponding t-statistics and *p*-values and the R value of the model. LMEs were conducted in MATLAB (R2020b, MathWorks).